TITLE

dArc1 controls sugar reward valuation in *Drosophila melanogaster*

AUTHORS

Sven Bervoets[1,2], Miles Solomon Jacob[1], Anita V. Devineni[3], Brennan Dale Mahoney[1], Kaelan R. Sullivan[2], Andrew R. Butts[1], Hayeon Sung[4], Jenifer Einstein[2], Mark M. Metzstein[5], Monica Dus[4], Jason D. Shepherd[2,*], Sophie Jeanne Cécile Caron[1,*,#].

[1]School of Biological Sciences, University of Utah, Salt Lake City, UT 84112, United States.

[2]Department of Neurobiology, University of Utah, Spencer Fox Eccles School of Medicine, Salt Lake City, UT 84112, United States.

[3]Department of Biology, Emory University, Atlanta, GA 30322, United States.

[4]Department of Molecular, Cellular and Developmental Biology, The University of Michigan, Ann Arbor, MI 48109, United States.

[5]Department of Human Genetics, University of Utah, Spencer Fox Eccles School of Medicine, Salt Lake City, UT 84112, United States

[*]Equal contribution

[#]Lead contact

ABSTRACT

The *Arc* genes — which include *Drosophila Arc1* and *Arc2* (*dArc*) — evolved from Ty3 retrotransposons and encode proteins that form virus-like capsids. These capsids enable a novel form of intercellular communication by transferring RNAs between cells. However, the specific neuronal circuits and brain processes Arc intercellular signaling regulates remain unknown. Here, we show that loss of both *dArc* genes in *Drosophila melanogaster* enhances associative learning in an appetitive conditioning paradigm, where flies associate an odor with sugar rewards. This increased learning performance arises from an increased valuation of sugar rewards: unlike wild-type flies, *dArc*$^{-/-}$ flies form abnormally strong associations even when the sugar reward is small or has no caloric value. We found that the γ5-dopaminergic neurons of the protocerebral anterior medial (PAM) cluster, which encode the positive valence of sugar rewards, show heightened activity in response to sucrose in *dArc*$^{-/-}$ flies. We further show that the learning phenotype of *dArc*$^{-/-}$ flies depends on the formation of capsids, underscoring a direct role for capsid-mediated Arc

signaling in sugar valuation. Our findings establish *dArc* genes as critical regulators of reward valuation in *D. melanogaster*, acting through a non-cell autonomous mechanism that relies on capsid-mediated communication between cells.

MAIN TEXT

The activity-regulated cytoskeletal-associated (*Arc*) gene was initially identified in mammals as an immediate early gene — rapidly induced by neuronal activity — that has critical roles in synaptic plasticity[1,2]. Two Arc genes, *dArc1* and *dArc2,* have been identified in schizophoran flies, including *Drosophila melanogaster*. Recent evidence indicates that Arc proteins can self-assemble into capsids, enabling the transfer of RNAs between neurons[3,4]. This non-synaptic signaling mechanism may represent a completely new mode of intercellular communication in nervous systems[5]. The ability to form capsids that can transfer RNAs between cells is an ancestral property of these proteins[4,6]. *Arc* genes evolved from Ty3 retrotransposons — a class of mobile genetic element — and exhibit high sequence homology to Gag domains, which form the capsids of retrotransposons and retroviruses[3,7,8]. However, it remains unclear whether capsid-mediated signaling is essential for the functions of *Arc* genes.

dArc1 and *dArc2* play diverse roles, influencing processes ranging from metabolism regulation to associative learning[9–11]. However, only *dArc1* has been linked to synaptic function at the larval neuromuscular junction, and its expression has been shown to increase in response to neuronal activity[12,4]. Structural analyses of dArc capsids have resolved their architecture at atomic resolution, identifying key domains for capsid assembly and RNA binding[6]. In the larval neuromuscular junction, dArc1 has been shown to transfer RNAs, including its own mRNA, from motor neurons to muscle cells, highlighting its capacity for intercellular RNA transport[4]. However, it remains unclear whether and how Arc signaling operates in the *Drosophila* brain. Here, we demonstrate that *dArc1* is required in the adult *Drosophila* brain for accurate valuation of sugar rewards during associative learning, and that this function relies on its ability to form capsids.

dArc1 is expressed in a subset of serotonergic neurons

To determine where dArc1 is expressed in the adult *Drosophila* brain, we performed immunostaining on the brains of five-day-old flies using custom polyclonal antibodies specific to dArc1 (Extended Data Fig. 1a). In brains immunostained for dArc1, we identified on average 29 $\pm$ 1 cells with dArc1 expression (Fig. 1a,b and Extended Data Fig. 1b). The somata of these cells are sparsely distributed in the anterior and posterior brain.

Using cell-type specific reporter transgenes, we found that dArc1 expression was restricted to neurons and not detected in glial cells (Fig. 1e). Immunostaining for the neuronal marker elav and the glial marker repo corroborated these findings (Extended Data Fig. 2a,b). Notably, approximately one-third of dArc1-expressing neurons co-expressed the *Trhn-GAL4* transgene, which labels all serotonergic neurons but not all serotonergic neurons express dArc1 (Fig. 1c-e). Four dArc1-positive serotonergic neurons were consistently observed in the suboesophageal zone, a taste processing center in the *D. melanogaster* brain (Fig. 1c,d). We did not detect dArc1 expression in dopaminergic, GABAergic, or octopaminergic neurons, and only a small subset of cholinergic and glutamatergic neurons showed dArc1 expression (Fig. 1e and Extended Data Fig. 2c,d). Thus Arc1-expressing neurons is a heterogeneous group of neurons that consists of serotonergic, cholinergic, and glutamatergic neurons as well as other unidentified neurons.

$dArc^{-/-}$ flies outperform $dArc^{+/+}$ flies in an appetitive conditioning paradigm

dArc1 and *dArc2* share high homology, with both encoding proteins capable of forming capsids[6]. To prevent compensatory effects from the deletion of only *dArc1*, we used CRISPR-mediated homologous recombination to generate fly lines in which the entire *dArc* locus, a region containing both *dArc1* and *dArc2*, was deleted ($dArc^{-/-}$ flies; Extended Data Fig. 3a). We also generated a control line, in which the *dArc* locus was left intact ($dArc^{+/+}$ flies). qPCR of cDNA, western blots of protein extracts, and immunostaining of brains confirmed the absence of *dArc1* and *dArc2* in $dArc^{-/-}$ flies (Extended Data Fig. 1a and Extended Data Fig. 3b-d). $dArc^{-/-}$ flies are viable, develop normally and are fertile. They display no visible morphological defects and have normal motor behavior (Extended Data Fig. 3e).

We used a well-established associative conditioning paradigm to test whether $dArc^{-/-}$ flies have learning defects[13,14] (Extended Data Fig. 4a). Flies were trained to associate an odor with a sucrose reward, and their memory was tested either 30 minutes (short-term memory) or 24 hours (long-term memory) after training. $dArc^{-/-}$ flies significantly outperformed $dArc^{+/+}$ flies in both when their memories were tested after 30 minutes or 24 hours, showing performance indices flies were almost twice as high as those of $dArc^{+/+}$ flies (Fig. 2a,b).

To determine whether this enhanced learning performance resulted in enhanced memory consolidation, we tested flies two, four, and seven days after training (Fig. 2b). After two days, the appetitive memory in $dArc^{+/+}$ flies was completely extinguished, while $dArc^{-/-}$ flies only weakly expressed the memory. However, after four days, the memories in both genotypes were entirely

extinguished, suggesting that memories do not persist longer in *dArc*$^{-/-}$ flies. To ensure that the difference in performance was not due to variation in sensory perception, we measured odor acuity and innate responses to sucrose and found it to be similar across genotypes and not due to metabolic defects such as abnormal fat mass (Extended Data Fig. 4b-i). Therefore, the enhanced learning of *dArc*$^{-/-}$ flies does not result from sensory defects and does not translate into enhanced memory persistence.

To determine whether the enhanced learning phenotype is specific to sucrose rewards or reflects more general defects in reward learning, we tested flies with different reward learning paradigms. We used water as an alternative appetitive reward by modifying the appetitive conditioning paradigm based on previous studies[15,16]. Flies were water-deprived for 20 hours before training, then a water reward was delivered during the training period. Flies were tested 30 minutes after training. We found that *dArc*$^{-/-}$ and *dArc*$^{+/+}$ flies performed similarly, showing no differences in performance or water preference (Fig. 2c and Extended Data Fig. 5a). This suggests that the defects in *dArc*$^{-/-}$ flies might be specific for the sugar reward pathway. To test whether other forms of learning are affected in *dArc*$^{-/-}$ flies, we trained flies in an aversive conditioning paradigm using electric shocks[14,17]. We observed a significant reduction in performance indices compared to *dArc*$^{+/+}$ flies when we tested short-term memory, but no differences when we tested long-term memory (Fig. 2d,e). Additionally, we observed a significant difference in the ability of *dArc*$^{-/-}$ flies to detect electric shocks, a sensory defect that may further contribute to impaired aversive learning (Extended Data Fig. 5b-c).

dArc$^{-/-}$ flies do not differ in their hunger and motivational states

The higher sugar reward learning performance indices observed in *dArc*$^{-/-}$ flies might result from a dysregulation of the mechanisms assessing nutritional status — *dArc*$^{-/-}$ flies might simply be hungrier than *dArc*$^{+/+}$flies — or from a dysregulation of the mechanisms that repress appetitive memories when flies are sated. In the first scenario, *dArc*$^{-/-}$ flies would constantly be in a heightened hunger state and might express their appetitive memories more readily than *dArc*$^{+/+}$ flies, leading to higher performance indices. However, *dArc*$^{-/-}$ flies did not show abnormal responses to sucrose: they did not show a greater preference for dwelling over sweet surfaces, nor did they exhibit an aberrant proboscis extension-reflex, suggesting that they were not hungrier than starved *dArc*$^{+/+}$ flies (Extended Data Fig. 4b-d). To investigate further possible differences in hunger state, we measured food intake in starved flies that were fed blue-dyed sucrose for two minutes, the same duration as the training phase in the appetitive conditioning paradigm

125 (Extended Data Fig. 4h). We found no significant differences in feeding initiation between the genotypes. Additionally, we detected no significant differences in triglyceride or protein levels between genotypes when fed a normal or high sucrose diet, suggesting that *dArc*$^{-/-}$ flies have similar fat mass and do not have a higher performance index because of lower energy stores (Extended Data Fig. 4i).

130 Sated flies are less motivated to show a preference for an odor they have learned to associate with a sucrose reward, as the expression of such appetitive memories is controlled by hunger state[18]. It is conceivable that the neuronal mechanisms that repress appetitive memories when flies are sated are defective in *dArc*$^{-/-}$ flies, leading to their enhanced performance in the sucrose reward conditioning paradigm. To explore this possibility, we trained *dArc*$^{+/+}$ and *dArc*$^{-/-}$
135 flies using sucrose rewards and tested their preference for the conditioned odor when flies were sated (Extended Data Fig. 6a). As expected, *dArc*$^{+/+}$ flies expressed appetitive memories only when starved. Similarly, *dArc*$^{-/-}$ flies expressed appetitive memories only when starved, suggesting that the mechanisms controlling the repression of appetitive memories in response to hunger state are intact.

140 **_dArc_$^{-/-}$ flies overvalue different types of sugar reward**

Appetitive associative memories are formed when the positive value of a stimulus, such as a sugar reward, is associated with a neutral stimulus, such as an odor, through learning. The higher performance indices observed with *dArc*$^{-/-}$ flies may result from defects in the valuation of the sugar reward. Flies value sugar rewards based on both taste and nutritional content: sugars that
145 taste sweet but lack nutritional content are not valued as highly as those that taste sweet and provide calories. When used in a conditioning paradigm, sweet-tasting sugars without caloric value typically lead to weaker memories than sweet-tasting sugars that provide nutritional value[19]. We used two different experimental assays to test whether *dArc*$^{-/-}$ flies value sugar rewards differently than *dArc*$^{+/+}$ flies. In the first set-up, we trained flies using arabinose, a sugar that tastes
150 sweet but has no caloric value, and tested their preference for the conditioned odor either immediately after training or 30 minutes later. *dArc*$^{-/-}$ flies showed enhanced learning compared to *dArc*$^{+/+}$ flies when trained with arabinose, forming memories that were almost as strong as those formed with sucrose (Fig. 3a and Extended Data Fig. 6b). In the second assay, we trained flies using lower concentrations of sucrose — 10 mM, 100 mM and 250 mM. Only *dArc*$^{-/-}$ flies were
155 able to learn at all concentrations and significantly outperformed *dArc*$^{+/+}$ flies when trained with 250 mM sucrose (Fig. 3b and Extended Data Fig. 6c). These experiments show that *dArc*$^{-/-}$ flies

outperform *dArc*$^{+/+}$ flies when trained with sugar rewards that have no or low caloric value, suggesting an overvaluation of sugar reward.

γ5 dopaminergic neurons in *dArc*$^{-/-}$ flies show aberrantly strong responses to sucrose

In *D. melanogaster*, *a*ssociative learning takes place in the mushroom body[20,21]. The Kenyon cells that make up the mushroom body encode odor identity and are connected to different mushroom body output neurons that mediate either attraction or aversion to specific stimuli. Reward valence is encoded by dopaminergic neurons, where positive stimuli activate the protocerebral anterior medial (PAM) neurons[22,23]. Sugar rewards activate the PAM neurons that innervate the β'2 and γ5 compartments of the mushroom body, while water rewards activate those innervating the γ4 compartment[23]. The sugar valuation defects in *dArc*$^{-/-}$ flies may be due to hyperactivation of the β'2 and γ5 PAM neurons in response to sugar. To test this possibility, we recorded sugar-evoked activity in starved flies using calcium imaging and two-photon microscopy. We used the *R58E02-GAL4* transgene to target expression to the PAM neurons and the *UAS-GCaMP* transgene to record odor-evoked calcium transients[24,25]. Calcium transients were recorded in the β'2, γ4 and γ5 compartments following stimulation with 100 mM sucrose solution. We observed weak stimulus-evoked responses in the γ4 compartment, which were similar in magnitude in *dArc*$^{+/+}$ or *dArc*$^{-/-}$ flies (Fig. 4a). In the β'2 compartment, we observed strong stimulus-evoked responses, but there was no significant difference between *dArc*$^{+/+}$ and *dArc*$^{-/-}$ flies (Fig. 4b). In contrast, we observed strong stimulus-evoked responses in the γ5 compartment, with significantly higher responses in *dArc*$^{-/-}$ flies compared to *dArc*$^{+/+}$ flies (Fig. 4c). These experiments show that *dArc*$^{-/-}$ flies have functional defects in a restricted subset of dopaminergic neurons — the γ5 PAM neurons — that encode the value of sugar rewards.

Capsid formation is necessary for dArc1 function in sucrose reward learning

dArc1 is expressed in a small number of neurons, most of which are serotonergic, but is not expressed in dopaminergic PAM neurons (Fig. 1 and Extended Data Fig. 2c,d). However, the defects we observed concern specific dopaminergic neurons, particularly the γ5 PAM neurons, raising the question of how dArc1 might exert its effect on these neurons. Previous studies have shown that dArc1 can self-assemble into virus-like capsids that are released in extracellular vesicles[4,3,6]. These observations suggest that dArc1 may affect dopaminergic neurons non-cell autonomously through the release of capsids by serotonergic neurons. To explore this possibility, we designed a dArc1 variant that cannot assemble into capsids (dArc1$^{\Delta capsid}$) (Fig. 5a) and tested

whether rescuing the expression of *dArc1* or *dArc1*$^{\Delta capsid}$ in serotonergic neurons could restore the enhanced learning phenotype observed in *dArc*$^{-/-}$ flies to *dArc*$^{+/+}$ levels. Purified dArc1$^{\Delta capsid}$ protein does not form capsids or oligomers (Fig. 5b-c, Extended Data Fig. 7a-c).

We tested whether rescuing the expression of *dArc1* or *dArc1*$^{\Delta capsid}$ could restore the enhanced learning phenotype observed in *dArc*$^{-/-}$ flies to *dArc*$^{+/+}$ levels. We generated *UAS* transgenes encoding either *dArc1* or *dArc1*$^{\Delta capsid}$. We targeted expression of either transgene to all neurons using the *nSynaptobrevin-GAL4* transgene (*nSyb-GAL4*) or we targeted expression specifically to serotonergic neurons using the *tryptophan-hydroxylase-GAL4* (*Trhn-GAL4*). Rescuing *dArc1* in all neurons restored the learning phenotype observed in *dArc*$^{-/-}$ flies to *dArc*$^{+/+}$ levels (Fig. 5d, Extended Data Fig. 8a). In contrast, expression of *dArc1*$^{\Delta capsid}$ did not affect the enhanced learning performance of *dArc*$^{-/-}$ flies, suggesting that capsid formation is necessary for *dArc1* function in appetitive learning. Similarly, we found that expression of *dArc1*, but not *dArc1*$^{\Delta capsid}$, in serotonergic neurons was sufficient to restore the learning phenotype observed in *dArc*$^{-/-}$ flies to *dArc*$^{+/+}$ levels (Fig. 5e). Expression of these transgenes in *dArc*$^{+/+}$ flies had no effect on learning performance (Extended Data Fig. 8b).

We confirmed the expression of both the *UAS-dArc1* and *UAS-dArc1*$^{\Delta capsid}$ transgenes in neurons using the dArc1 antibody, which also recognizes dArc1$^{\Delta capsid}$ (Fig 5f and Extended Data Fig. 8a). Notably, the expression patterns differed between *dArc*$^{-/-}$;*Trhn-GAL4*;*UAS-dArc1* and *dArc*$^{-/-}$;*Trhn-GAL4*;*UAS-dArc1*$^{\Delta capsid}$ flies. In *dArc*$^{-/-}$;*Trhn-GAL4*;*UAS-dArc1* flies, dArc1 staining was distributed throughout serotonergic neurons, with distinct puncta observed along neuronal processes. In *dArc*$^{-/-}$;*Trhn-GAL4*;*UAS-dArc1*$^{\Delta capsid}$ flies, dArc1 staining was confined to the somata, suggesting that trafficking or secretion of dArc1$^{\Delta capsid}$ is disrupted.

DISCUSSION

Our genetic and neurobiological experiments show that the retrotransposon-derived gene *dArc1* regulates associative learning by dampening the valuation of sugar rewards. Flies lacking *dArc1* overvalue sugar, leading to enhanced learning in an appetitive conditioning paradigm. This behavior is accompanied by hyperactivation of the γ5 PAM neurons in response to sucrose, suggesting that *dArc1* may regulate reward valuation by specifically modulating the activity of these neurons. Expressing *dArc1* in all serotonergic neurons corrected the enhanced learning phenotype in *dArc*$^{-/-}$ flies, while expression of a capsid assembly-deficient variant did not. These

findings highlight the importance of dArc1 capsids, suggesting that this property is essential for its role in sugar valuation and associative learning, likely through intercellular signaling.

Such an enhanced learning phenotype is generally not known from studies of *Drosophila* neurogenetics and this may seem counterintuitive — why would the fly brain require a mechanism to suppress learning? However, this may make sense in the light of the nutritional physiology of *D. melanogaster*: Adult flies feed on fermenting fruit — an ephemeral food source that is rich in sugars — but also require proteins, provided by yeast colonizing fruit, in particular during egg production[26]. Excess carbohydrate consumption in *D. melanogaster* was shown to disrupt metabolic homeostasis in adults, impairing reproductive success and reducing lifespan[27–29]. By dampening dopaminergic reward signaling in response to sugar, Arc1 signaling may ensure that flies do not become overly dependent on sugar-rich food sources and continue to seek out a balanced diet. By contrast, when sugar is scarce, and Arc signaling down-regulated, carbohydrate rich food sources can be learned easily.

dArc and *mammalian Arc* (*mArc*) have an unusual evolutionary origin: they are independently derived from Ty3-type retrotransposons and encode proteins that form virus-like capsids that can travel between cells[3,4]. Here, we show that capsid formation is necessary for *dArc1* function in the fly brain. This raises the question of how this unusual mechanism of neuromodulation regulates sugar reward valuation. One possibility is that dArc1 signaling may induce state-dependent changes in target neurons that alter the ability to induce mechanisms of synaptic plasticity known from studies of learning in flies[30]. As dArc1 is expressed in serotonergic neurons — including those in the suboesophageal zone, which play key roles in modulating internal states[31] — capsid signaling may integrate nutritional information over time, promoting adaptive plasticity in the neuronal circuits involved in associative learning. Further elucidation of dArc1 signaling mechanisms and — in particular the nature and function of the RNA cargoes transferred — will help address these questions.

The *Arc* genes represent a striking case study of evolutionary innovation in genomes by repurposing mobile genetic elements to enable vital organismal functions through unusual virus-like molecular mechanisms. *Arc* genes are found in two evolutionarily very successful lineages of animals: in tetrapod vertebrates, which count around 30,000 species, and in schizophoran flies, which count over 55,000 species[32,33]. Although this phylogenetic distribution indicates two independent integration events, both *dArc1* and *Arc* function in neuronal plasticity and appear to employ a similar capsid-dependent mechanism of signaling[3,4]. As transposon-derived sequences

250 make up large swaths of animal genomes — over 50% of the human genome — Arc genes provide a window into the function and evolution of this 'dark matter of the genome'[34].

ACKNOWLEDGMENTS

We thank members of the Caron and Shepherd laboratories for comments on the manuscript and discussions of the project. We are grateful to Dr. Adrian Rothenfluh for meaningful discussions on
255 throughout the development of this project. We extend our heartfelt thanks to Dr. Florian Maderspacher for entertaining countless discussions on Arc and offering invaluable editorial insights. We also want to acknowledge Dr. Simon Erlendsson (University of Copenhagen) and Dr. John Briggs (Max Planck Institute of Biochemistry) for their help designing *dArc1*$^{\Delta capsid}$; Dane Larsen for the initial characterization of the dArc1 antibody; Adam Lin and Sylvia Yang for
260 preparation of the standard cornmeal agar medium; Hayley Smihula and Lia Beatty for assistance with general laboratory concerns; the Cell Imaging Core at the University of Utah for use of the Zeiss LSM 880 microscope; and the Electron Microscopy Core at the University of Utah for use of the ThermoFisher JEOL-JEM 1400 microscope.

This work was initially funded by a Seed Grant awarded by the Neuroscience Initiative at
265 the University of Utah (S.J.C.C., M.M.M. and J.D.S. and has been funded thereafter by grants from the National Institute for Neurological Disorders and Stroke (R01 NS 106018, R01 NS 1079790 and R01 NS 115716) and the National Science Foundation (IOS 2042397). Further financial support was provided by the Research Scholar Award (M.S.J. and B.D.M.), the University Research Opportunities Program (M.S.J.), the Chan-Zuckerberg Initiative (Ben Barres Early
270 Acceleration Award; J.D.S.), the Jon M. Huntsman Presidential Endowed Chair Fund (J.D.S.) and the Georges S. and Dolores Eccles Foundation (S.J.C.C.).

AUTHOR CONTRIBUTIONS

S.B., J.D.S. and S.J.C.C. conceived the project. S.B., J.D.S. and S.J.C.C. wrote the manuscript with input from all other authors. S.B. generated the UAS transgenic lines, performed and
275 analyzed behavioral experiments (conditioning paradigms, feeding assay), performed expression analyses by qPCR and western blot, and generated the *dArc*$^{-/-}$ flies. M.S.J performed and analyzed behavioral experiments (conditioning paradigms). A.V.D. collected and analyzed the calcium imaging data. B.D.M. performed expression analyses by immunocytochemistry. K.R.S. performed protein purification and electron microscopy. A.R.B. performed expression analyses by
280 immunocytochemistry and behavioral experiments (negative geotaxis assays, feeding assays).

H.S. performed behavioral experiments (proboscis extension reflex), electrophysiological recordings, and metabolic assays under the supervision of M.D. J.E. and M.M.M. generated the *dArc*$^{+/+}$ and *dArc*$^{-/-}$ flies. J.D.S and S.J.C.C obtained funding for the project.

DECLARATION OF INTERESTS

The authors declare no competing interests.

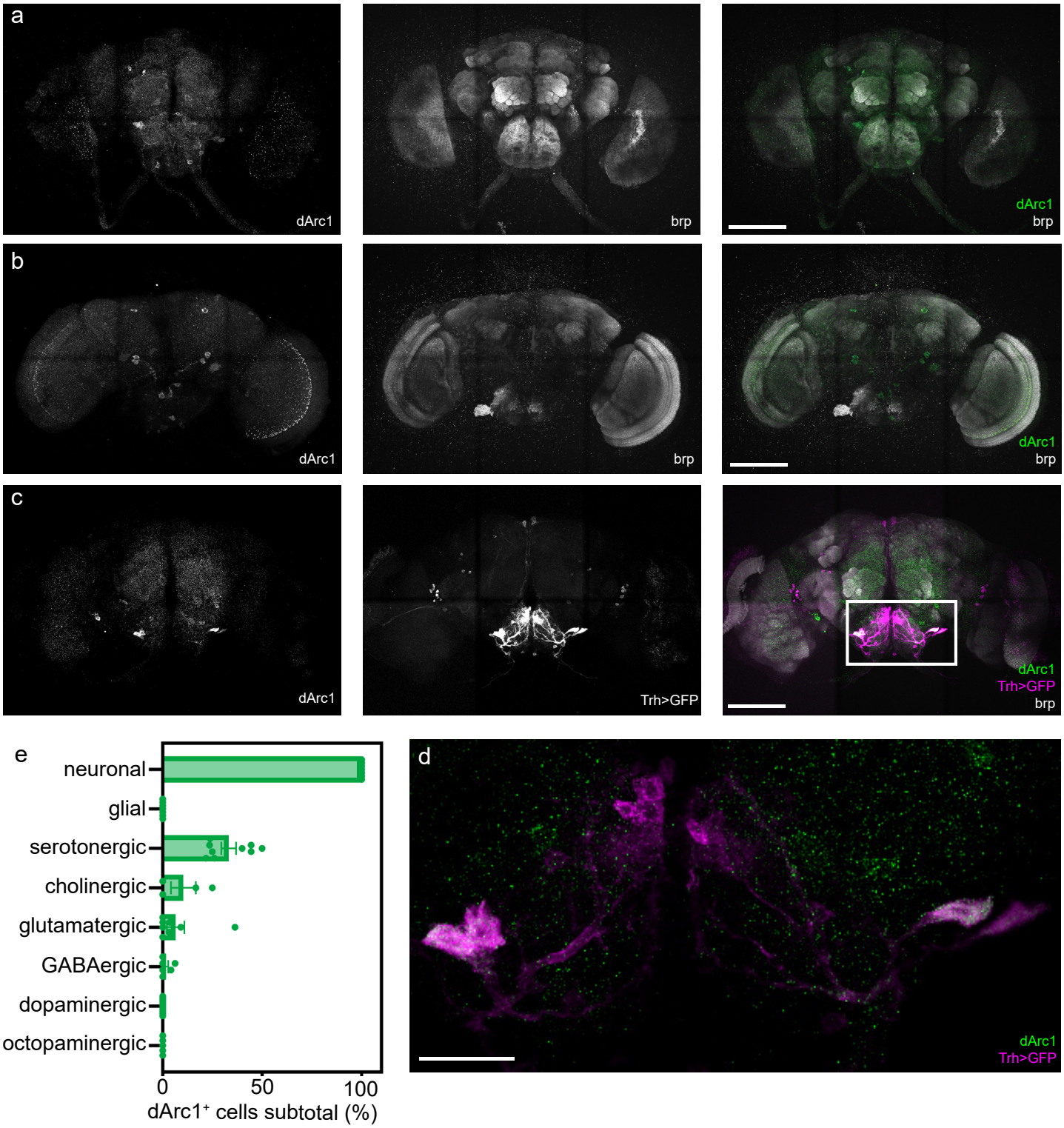
a
dArc1
brp
dArc1
brp
b
dArc1
brp
dArc1
brp
c
dArc1
Trh>GFP
dArc1
Trh>GFP
brp
e
neuronal
glial
serotonergic
cholinergic
glutamatergic
GABAergic
dopaminergic
octopaminergic
0
50
100
dArc1⁺ cells subtotal (%)
d
dArc1
Trh>GFP

Figure 1 | dArc1 is expressed in a subset of serotonergic neurons.

(a) The brains of *dArc*$^{+/+}$ and *dArc*$^{-/-}$ flies were immunostained and imaged using antibodies against the neuropil marker bruchpilot (white) and dArc1 (green) on the anterior and

(b) posterior side. Scale bars are 100 μm.

(c) The brain of a *Trhn*-GAL4;UAS-GFP fly was immunostained and imaged using antibodies against bruchpilot (white) and dArc1 (green) and intrinsic GFP fluorescence signal (magenta). Scale bar is 100 μm.

(d) Zoomed-in image showing the colocalization of dArc1 (green) in the serotonergic neurons (magenta) of the suboesophageal zone. Scale bar is 50 μm.

(e) The brains of flies carrying a GAL4 transgene and the UAS-GFP transgene were immunostained and imaged using antibodies against dArc1 and intrinsic GFP signal; cells were typed based on whether they express GFP and the fraction of the dArc1-expressing cells belonging to a given type was measured ($n \geq 4$ flies). Subjects were mixed sex. Bar charts are presented as means ± s.e.m.

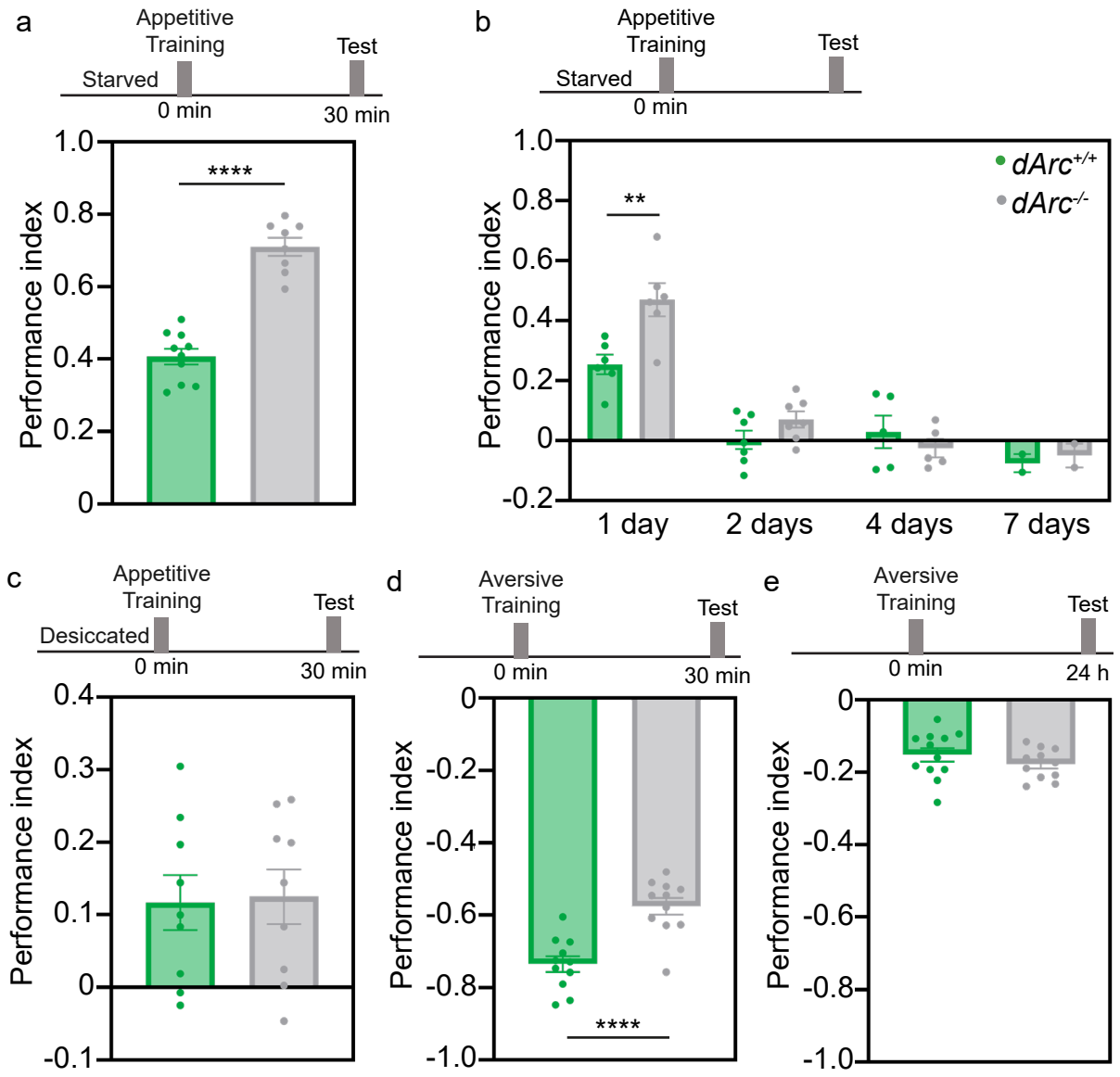
a
Appetitive Training
Test
Starved
0 min
30 min
Performance index
1.0
0.8
0.6
0.4
0.2
0
****
b
Appetitive Training
Test
Starved
0 min
Performance index
1.0
0.8
0.6
0.4
0.2
0
-0.2
**
dArc+/+
dArc-/-
1 day
2 days
4 days
7 days
c
Appetitive Training
Test
Desiccated
0 min
30 min
Performance index
0.4
0.3
0.2
0.1
0
-0.1
d
Aversive Training
Test
0 min
30 min
Performance index
0
-0.2
-0.4
-0.6
-0.8
-1.0
****
e
Aversive Training
Test
0 min
24 h
Performance index
0
-0.2
-0.4
-0.6
-0.8
-1.0

305 **Figure 2 | *dArc*$^{-/-}$ flies show enhanced sugar reward learning.**

(a) Flies were starved for 20 hours and subjected to an appetitive association paradigm using sucrose and tested after 30 minutes. ($n \geq 8$ groups of flies, Unpaired t-test).

(b) Flies were starved for 20 hours and were subjected to an appetitive association paradigm using sucrose and tested after 1, 2, 4, or 7 days. ($n \geq 2$ groups of flies, Two-way ANOVA).

310 (c) Flies were desiccated for 20 hours and were subjected to an appetitive association paradigm using water and tested after 30 minutes. ($n \geq 9$ groups of flies, Unpaired t-test).

(d) Flies were subjected to an aversive association paradigm using a single shock regime and tested after 2 minutes. ($n \geq 10$ groups of flies, Unpaired t-test).

(e) Flies were subjected to an aversive association paradigm using multiple spaced shock

315 regimes and tested after 24 hours. ($n \geq 11$ groups of flies, Unpaired t-test). Subjects were mixed sex. Bar charts are presented as means ± s.e.m.

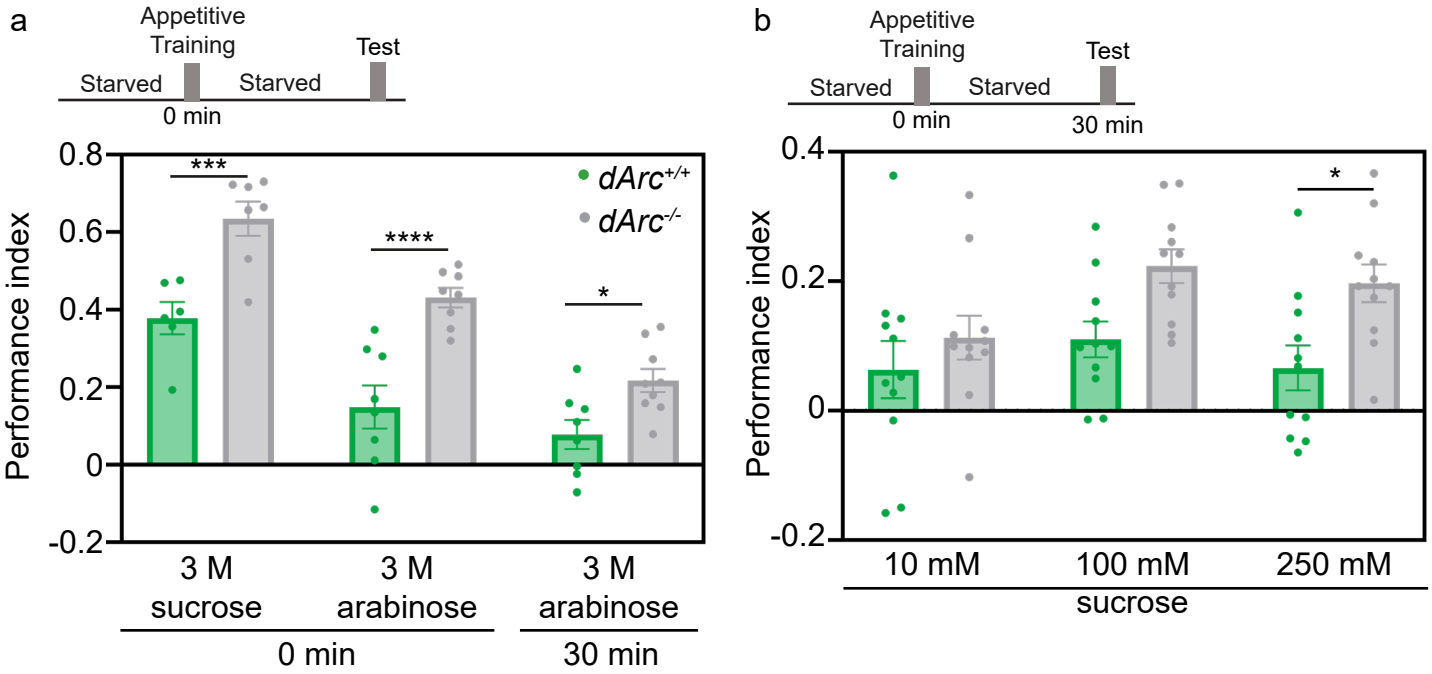
a
Appetitive Training
Test
Starved
Starved
0 min
Performance index
0.8
0.6
0.4
0.2
0
-0.2
***
****
*
dArc+/+
dArc-/-
3 M sucrose
3 M arabinose
3 M arabinose
0 min
30 min
b
Appetitive Training
Test
Starved
Starved
0 min
30 min
Performance index
0.4
0.2
0
-0.2
*
10 mM
100 mM
250 mM
sucrose

320 **Figure 3 | dArc$^{-/-}$ flies overvalue sugar rewards.**

(a) Flies were starved for 20 hours and were subjected to an appetitive association paradigm using sucrose or the non-caloric sugar arabinose. The flies were then tested after 2 minutes for their immediate learning or 30 minutes for their short-term memory. ($n \geq 6$ groups of flies, Two-way ANOVA).

325 (b) Flies were starved for 20 hours and were subjected to an appetitive association paradigm using different concentrations of sucrose and tested after 30 minutes. ($n \geq 7$ groups of flies, Two-way ANOVA). Subjects were mixed sex. Bar charts are presented as means ± s.e.m.

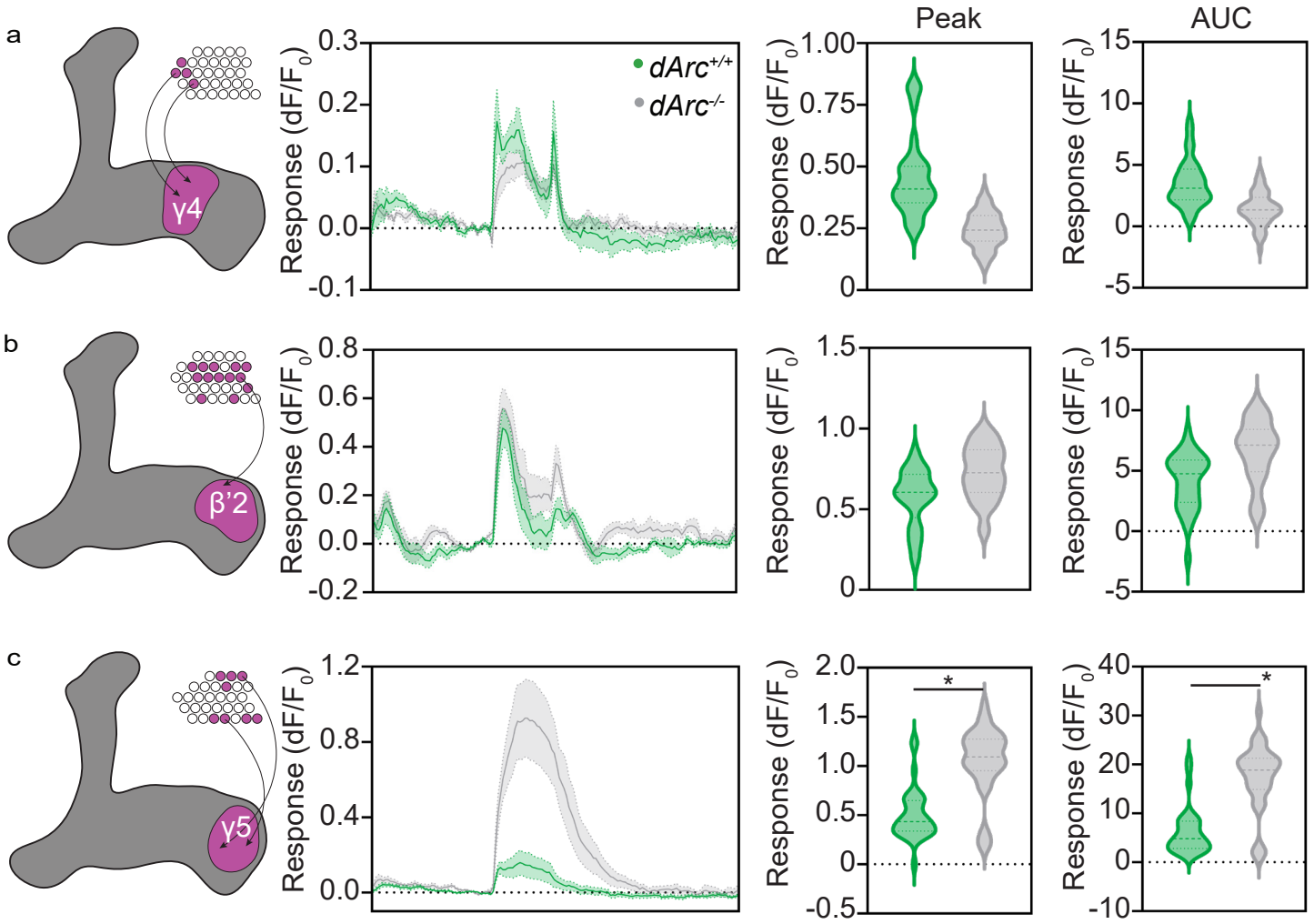
a
γ4
dArc+/+
dArc-/-
Response (dF/F0)
Peak
AUC
b
β'2
c
γ5
*

Figure 4 | dArc$^{-/-}$ flies have enhanced sugar responses in γ5 dopaminergic PAM neurons.

(a) Starved flies expressing *UAS-GCaMP7f* in the protocerebral anterior medial dopaminergic neurons (*R58E02-GAL4*) were subjected to sucrose and their responses were measured in the γ4 dendritic arbors of the mushroom body. Total (AUC) and peak response of each response is quantified. (n ≥ 7 flies, 12-58 trials, nested t-test).

(b) Starved flies expressing *UAS-GCaMP7f* in the protocerebral anterior medial dopaminergic neurons (*R58E02-GAL4*) were subjected to sucrose and their responses were measured in the β'2 dendritic arbors of the mushroom body. Total (AUC) and peak response of each response is quantified. (n ≥ 5 flies, 8-34 trials, nested t-test).

(c) Starved flies expressing *UAS-GCaMP7f* in the protocerebral anterior medial dopaminergic neurons (*R58E02-GAL4*) were subjected to sugar and their responses were measured in the γ5 dendritic arbors of the mushroom body. Total (AUC) and peak response of each response is quantified. (n ≥ 10 flies, 16-36 trials, nested t-test). Subjects were mated females. Line graphs are presented as means ± s.e.m. Violin plots show the median (dashed line) and quartiles (dotted line).

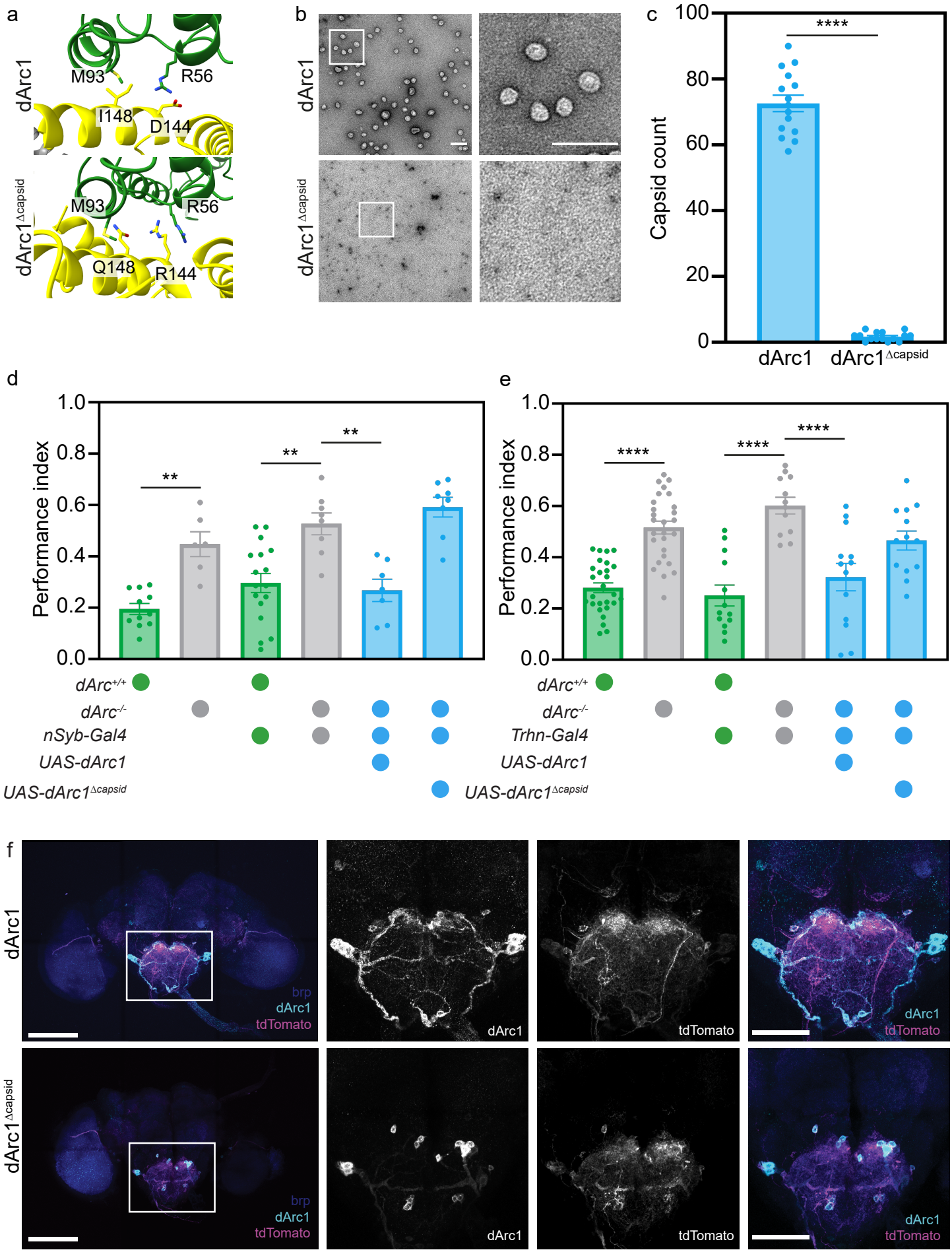
a
dArc1
M93
R56
I148
D144
dArc1Δcapsid
M93
R56
Q148
R144
b
dArc1
dArc1Δcapsid
c
Capsid count
100
80
60
40
20
0
****
dArc1
dArc1Δcapsid
d
Performance index
1.0
0.8
0.6
0.4
0.2
0.0
**
**
**
dArc+/+
dArc-/-
nSyb-Gal4
UAS-dArc1
UAS-dArc1Δcapsid
e
Performance index
****
****
****
dArc+/+
dArc-/-
Trhn-Gal4
UAS-dArc1
UAS-dArc1Δcapsid
f
dArc1
brp
dArc1
tdTomato
dArc1
tdTomato
dArc1
tdTomato
dArc1Δcapsid
brp
dArc1
tdTomato
dArc1
tdTomato
dArc1
tdTomato

Figure 5 | dArc1 capsids regulate sugar reward learning.

350 (a) Visualization of the capsomer interface of two individual dArc1 proteins (green and yellow) indicating the introduced mutations. Colors on the displayed amino acid side chains indicate oxygen (red), nitrogen (blue), and sulfur (yellow).

(b) Negative stain EM of dArc1 or dArc1$^{\Delta capsid}$ proteins.

(c) Mean capsid counts from an electron microscope grid (n = 15 grid locations, Unpaired t-test)

355 (d) Flies starved for 20 hours expressing either dArc1 or dArc1$^{\Delta capsid}$ in all neurons (*nSyb-GAL4*) were subjected to an appetitive association paradigm using sucrose and tested after 30 minutes. (n ≥ 6 groups of flies, One-way ANOVA).

(e) Flies starved for 20 hours expressing either dArc1 or dArc1$^{\Delta capsid}$ in all serotonergic neurons (*Trhn-GAL4*) were subjected to an appetitive association paradigm using sucrose and tested
360 after 30 minutes. (n ≥ 12 groups of flies, One-way ANOVA).

(f) The brains of *dArc1/2*$^{-/-}$ flies expressing dArc1 and dArc1$^{\Delta capsid}$ proteins in all serotonergic neurons (*Trhn-GAL4*) labeled with *UAS-tdTomato* were immunostained using antibodies against the neuropil marker brp (blue), dArc1 (cyan), and mtdTomato (magenta). Shown is the anterior side of the brain and a zoom in of the suboesophageal zone. Scale bars are 100 μm.
365 Subjects were mixed sex. Bar charts are presented as means ± s.e.m.

MATERIALS AND METHODS

Fly stocks

370 Flies (*Drosophila melanogaster*) were fed on standard cornmeal agar medium and raised in a controlled environmental chamber (Percival Scientific, Inc.) that maintains a temperature of 25°C and 60% humidity under a 12 hours light-12 hours dark cycle. Crosses were set up and reared under the same conditions. The strains used in this study are described in the table below.

Transgene(s)	Source	Identifier
y[1] M{GFP[E.3xP3]=vas-Cas9.RFP-}ZH-2A w[1118]	Bloomington Drosophila Stock Center	55821
y1w67c23;sna[Sco],[Crew]DHI/CyO;;	Bloomington Drosophila Stock Center	1092
w1118;;repo-Gal4/TM3,Sb[1]	Bloomington Drosophila Stock Center	7415
P{w[+mC]=GAL4-elav.L}2/CyO	Bloomington Drosophila Stock Center	8765
w[*];;Trhn-Gal4	Rothenfluh lab	
w[*]; P{w[+mC]=ChAT-GAL4.7.4}19B P{w[+mC]=UAS-GFP.S65T}Myo31DF[T2]	Bloomington Drosophila Stock Center	6793
w[1118]; P{w[+mW.hs]=GawB}VGlut[OK371]	Bloomington Drosophila Stock Center	26160
P{w[+mC]=Gad1-GAL4.3.098}2/CyO	Bloomington Drosophila Stock Center	51630
w;;[TH-GAL4]3;*	Bloomington Drosophila Stock Center	8848
yw;[Tdc2-GAL4]/CyO;MKRS/TM2;	Bloomington Drosophila Stock Center	9313
w[*];P{y[+t7.7]w[+mC]=10XUAS-IVS-mCD8::GFP}attP2	Bloomington Drosophila Stock Center	32185
yw1118;;[R58E02-GAL4]attP2;	Bloomington Drosophila Stock Center	41347
w118;;[20XUAS-IVS-jGCaMP7f]VK5;	Bloomington Drosophila Stock Center	79032
y[1] w[*]; P{w[+m]=nSyb-GAL4.S}3*	Bloomington Drosophila Stock Center	51635
w[*];P{y[+t7.7]w[+mC]=10XUAS-IVS-myr::tdTomato}attP2	Bloomington Drosophila Stock Center	32221

375 **Generation of *dArc*$^{-/-}$ flies**

dArc$^{-/-}$ flies were generated using CRISPR/Cas9-mediated genomic engineering, following an established protocol[35,36]. Briefly, two guide RNAs (gRNAs) were designed to target various regions of *dArc1* and *dArc2* (gRNA1-2) and were evaluated for specificity and off-target effects using the CRISPR Target Finder tool (http://targetfinder.flycrispr.neuro.brown.edu/). These gRNA
380 sequences were cloned into the pU6-BbsI-chiRNA plasmid and sequence-verified. Homology arms of about 1 kb flanking the Cas9 cut sites were synthesized as gene blocks (IDT) and cloned into the pHD-DsRedattP plasmid, followed by sequence verification. The gRNAs and homology repair plasmids were co-injected into *vas-Cas9* transgenic embryos (Bestgene). Adult flies were backcrossed to *w*^{1118} flies. Mutant chromosomes were identified using the dsRed marker — which
385 was under the *3xP3* promoter and therefore visible in adult eyes — and isolated using the balancer chromosome *CyO*. The resulting *dArc*$^{-/-;DsRed}$ flies were crossed to flies expressing Cre recombinase (*Cre*) to excise the DsRed marker, yielding the *dArc*$^{-/-}$ flies used throughout this study. *dArc*$^{-/-}$ flies were validated by PCR using primers flanking the targeted region. The control line, *dArc*$^{+/+}$ flies, was established by isolating the second chromosome from *vas-Cas9* flies.

Oligonucleotide	Sequence
gRNA1 (sense)	cttcgcagttccacgcaaccacttg
gRNA1 (antisense)	aaaccaagtggttgcgtggaactgc
gRNA2 (sense)	cttcgggtatgctctcccggtact
gRNA2 (antisense)	aaacagtaccgggagagcataccc
PCR_dArc_CRISPR_F	taacgtctagaagggctgagac
PCR_dArc_CRISPR_R	tatcgatgctttgctgaacc

390

Generation of transgenic flies

The *UAS-dArc1* transgene was generated using Gibson cloning, following previously described protocols[37,38]. Briefly, *dArc1*, including its 3'-UTR, was cloned into the pUASt-attB plasmid (DGRC Stock 1419; https://dgrc.bio.indiana.edu/stock/1419; RRID:DGRC_1419) using primers with 30
395 base pairs homology arms. The construct was sequence-verified. The plasmid was inserted into the attPVK00033 site using PhiC31-mediated recombination[39]. Transgenic flies were identified by

the presence of the mini-white marker and isolated using the balancer chromosome *TM6B*. Point mutations were introduced in the pUASt-attB-dArc1 plasmid to generate the *UAS-dArc1*^{Dcapsid} transgene (Genescript). The mutated plasmids were sequence-verified. The plasmid was inserted in the attPVK00033 site using PhiC31-mediated recombination. Transgenic flies were identified by the presence of the mini-white marker and isolated using the balancer chromosome *TM6B*.

Oligonucleotide	Sequence
GIBSON_dArc1_UTR_F	acaaagatccccgtttctgagtttaatggttgttttctagt
GIBSON_pUASTattB_F	tcagaaacggggatctttgtgaaggaaccttacttctgt
GIBSON_dArc1_R	agggaattgggaaaatggcccagcttacacagat
GIBSON_pUASTattB_R	ggccattttcccaattccctattcagagttctcttc

Generation of Arc1 and Arc2 antibodies

Custom dArc1 antibodies were generated by the Proteintech Group. *dArc1* was cloned into the pGEX-4T1 plasmid. The GST-dArc1 fusion protein was purified and used to immunize two rabbits. Four booster immunizations were administered before the final bleed was collected from each rabbit. The custom antibodies were then affinity-purified using 6xHis-dArc1 and stored in 10% glycerol. Custom dArc2 antibodies were generated by ThermoFisher. A dArc2 peptide was synthesized (CKTFRELLDRGRTVERTRH) and used to immunize two guinea pigs. Three booster immunizations were administered before the final bleed was collected from each guinea pig. The custom antibodies were then affinity-purified using the dArc2 peptide and stored in 1x PBS with 0.05% NaN_3.

Immunohistochemistry

The brains of one to five day-old flies were dissected in saline and fixed in PFA for 45 min at room temperature, washed five times in PBST at room temperature, blocked in PBST-NGS for 30 min at room temperature, and incubated with different primary antibodies at 4°C overnight. Depending on the experiment, different antibodies were used at different concentrations (see table below). On the following day, brains were washed four times in PBST and incubated in secondary antibodies at 4°C overnight. Different secondary antibodies were used (see table below). On the following day, brains were washed four times in PBST and mounted on a slide (Fisher Scientific)

using the mounting media VECTASHIELD (Vector Laboratories Inc.). The neuropils were identified by comparing the confocal images with the adult brain template available in the FlyWire Codex (https://codex.flywire.ai/app/neuropils)[40,41].

Antibody	Concentration	Source
Rabbit anti-dArc1	1:1000	This study
AlexaFluor-546 goat-anti-rabbit	1:500	Life technologies
AlexaFluor-488 goat-anti-rabbit	1:500	Life technologies
Mouse anti-brp (nc82)	1:20	DSHB
AlexaFluor-633 goat-anti-mouse	1:500	Life technologies
AlexaFluor-546 goat-anti-mouse	1:500	Life technologies
Rat anti-tdTomato (16D7)	1:500	Kerafast
Alexa Fluor 568 goat-anti-rat	1:500	Life technologies

425 **Confocal image acquisition and analysis**

All confocal images were collected on LSM880 confocal microscope (Zeiss). For imaging whole brains, each sample was imaged using a Plan-Apochromat 40X/1.3 Oil M27 objective lens. First, the entire brain was divided into six tiles, each tile was imaged separately (voxel size = 0.21 µm by 0.21 µm by 0.44 µm) and then stitched together using the Stitch function of the Zen microscope
430 software (Zeiss). All confocal images were handled using the Fiji software[42]. All figure panels are maximum intensity projection of confocal stacks or sub-stacks.

Conditioning paradigms

Aversive and appetitive conditioning paradigms were performed following previously described protocols that use a T-maze[15,16,43,44]. Both paradigms consist of a training phase and a testing
435 phase. Each experiment was carried out on a group of 60 to 100 flies. In general, flies were selected prior to an experiment without sedation, except when selecting for the correct genotype. In such cases, flies were allowed to recover from anaesthesia for at least one full day. For the aversive paradigms, flies were kept on standard cornmeal fly food before the training phase. For

the appetitive paradigms, flies were kept on 1% agar for 20 hours prior to the training phase. The T-maze was used to train and test flies. In this T-maze, odors (4-methylcyclohexanol or 3-octanol; Sigma-Aldrich) were delivered through an air-flow that was held stable at 0.750L per minute. Odors were diluted in light mineral oil (Sigma-Aldrich), and the approximate concentration used in each experiment was ~$1:10^{-3}$ concentration. Odor concentrations were optimized to achieve a balanced distribution of naïve flies between the two arms of the T-maze prior to the training phase.

In the short-term appetitive conditioning paradigm, starved flies were initially placed in a tube containing an air-dried piece of paper (US^-) while exposed to an odor (CS^-) for two minutes, followed by a stream of unscented air for 30 seconds. Flies were transferred to a different tube containing a piece of paper with air-dried sugar (sucrose or arabinose; US^+) or a paper with dissolved sucrose in 1% agar (for different concentrations of sucrose; US^+) while exposed to another odor (CS^+) for two minutes, followed by a stream of unscented air for 30 seconds. Trained flies were returned to their original vial for the indicated time before the testing phase. In the long-term appetitive conditioning paradigm, flies were kept at 18°C before being tested.

In the short-term appetitive conditioning paradigm that used water as the reward, flies were desiccated by being kept in a tube with a piece of paper with air-dried sugar for 20 hours. Desiccated flies were then placed in a tube containing an air-dried piece of paper (US^-) while exposed to an odor (CS^-) for two minutes, followed by a stream of unscented air for 30 seconds. Flies were transferred to a different tube containing a wet piece of paper (US^+) while exposed to another odor (CS^+) for two minutes, followed by a stream of unscented air for 30 seconds. Flies were returned to their original vial for the indicated time before the testing phase.

In the short-term aversive conditioning paradigm, flies were placed in a copper-lined tube and exposed to an odor (CS^+) while receiving twelve 1-second 90V shocks over one minute (US^+), followed by a stream of unscented air for 45 seconds. Flies were then exposed to a second odor (CS^-) without electric shocks (US^-), followed by another stream of unscented air for 45 seconds. In the long-term aversive conditioning paradigm, flies underwent six training sessions, each consisting of twelve 1-second 90V shocks given over one minute, with a 15-minute interval between sessions. Flies were returned to their original vial for the indicated time before the testing phase.

During the testing phase for both the appetitive and aversive conditioning paradigms, trained flies were given the choice to enter one of two tubes in a T-maze: one scented with the conditioned odor previously paired with an appetitive reward or punitive shocks (CS^+) and the

other tube was scented with the conditioned odors that was not paired with an appetitive reward or punitive shocks (CS^-); flies had two minutes to make a choice. The flies located in each tube were collected and placed at -80°C at the end of the experiment. The number of flies in each tube was counted, and the performance index was calculated using the following formula: $PI = \frac{(CS+-CS-)}{(CS++CS-)}$. Flies that did not make a choice were discarded.

Calcium imaging

Calcium imaging experiments were performed using similar methods as previously described[45]. Flies were immobilized on their backs using a piece of clear tape in an imaging chamber. Fine strands of tape were used to restrain the legs, secure the head, and immobilize the proboscis in an extended position. A dorsal imaging window was cut in the fly cuticle. Images were collected using a two-photon laser scanning microscope (Investigator, Bruker) equipped with an ultra-fast Ti:Sapphire laser (Ultra II, Coherent) modulated by pockel cells (Conoptics). The excitation wavelength was 925 nm. Emitted photons were collected with a GaAsP photodiode detector (Hamamatsu) through a 20X water-immersion objective (Olympus). Images were acquired using the microscope software (PrairieView, Bruker). Imaging planes were chosen for optimal dendritic signal of each dopaminergic compartment in the mushroom body. Images were acquired at 512 by 512 pixels with a scanning rate of ~5 Hz.

Taste stimuli were delivered as drops to the labellum using a custom-built solenoid pinch valve system controlled by a MATLAB software through a data acquisition device (Measurement Computing). Solenoid pinch valves (Cole Parmer) were briefly opened (30-50 milliseconds) to create a small liquid drop at the end of a glass capillary. The capillary was positioned such that the drop made contact with the labellum. The drop was removed after five seconds by a vacuum line controlled by a solenoid pinch valve. Proper delivery of the drop was monitored using a side-mounted camera (FLIR Blackfly), which visualized the fly and the capillary. At least eight trials were conducted, with a minimum rest period of one minute between trials to avoid habituation. The taste stimulus used in all recordings was 100 mM sucrose. Only flies that displayed signs of health and activity — such as abdomen or proboscis movement — were included.

Calcium transients were analyzed using custom MATLAB (MathWorks) codes. Movement between individual images corrected, within and across trials for the same fly. Calcium transients ($\Delta F/ F_0$) were calculated by measuring the average fluorescence before and during stimulation

(F_0: four seconds prior to stimulus onset, F: three seconds during stimulus delivery). Data were pooled for each fly across trials and hemispheres for each imaged compartment.

Design of the dArc1$^{\Delta capsid}$ variant

The structure of dArc1 capsids, previously resolved by cryo-electron microscopy, was used to design the dArc1$^{\Delta capsid}$ variant. To disrupt the tertiary interactions between pentamers and hexamers necessary for capsid assembly, without altering the structure of the monomeric subunits, the aspartic acid at position 144 was substituted with an arginine and the isoleucine at position 148 with a glutamine. dArc1 and dArc1$^{\Delta capsid}$ were expressed in *Escherichia coli* and purified using glutathione S-transferase (GST) affinity purification followed by size exclusion chromatography. The purified dArc1 protein eluted early in the void fraction, indicating the presence of high molecular weight species, such as capsids. In contrast, the dArc1$^{\Delta capsid}$ protein eluted in later fractions, suggesting a lack of high molecular weight species (Extended Data Fig. 7a-c). The void fractions was imaged using negative stain electron microscopy.

Protein structure prediction

Protein structure predictions were performed using the Alphafold3 server (https://golgi.sandbox.google.com/about)[46]. The protein sequences of dArc1 and dArc1$^{\Delta capsid}$ were used. The molecule type was set at protein with five copies of the protein without any post-translational modifications. The output was visualized using the chimeraX software (https://www.rbvi.ucsf.edu/chimerax)[47].

Protein purification

GST-tagged proteins were purified from *Escherichia coli* Rosetta 2 BL21 competent cells as previously described[3]. Starter bacterial cultures were grown overnight at 37°C in LB medium supplemented with ampicillin and chloramphenicol. Large-scale 500 mL cultures were inoculated with the starter cultures in ZY auto-induction medium. These cultures were grown to an optic density of 600 nm of 0.6–0.8 at 37°C with shaking at 160 rpm, then shifted to 18°C with shaking at 180 rpm for 16–20 hours. Cultures were pelleted at 4000x*g* for 15 minutes at 4°C, and the resulting pellets were resuspended in 25 mL of lysis buffer (500 mM NaCl, 50 mM Tris, 5% glycerol, 1 mM DTT, pH 8.0) before being flash-frozen in liquid nitrogen. Frozen pellets were thawed in a 37°C water bath and brought to a final volume ratio of 1 g pellet:10 mL lysis buffer, supplemented with DNase, lysozyme, and a complete protease inhibitor cocktail (Roche).

Resuspended lysates were sonicated for six 45-second pulses at 90% duty cycle and then centrifuged at 21,000x*g* for 75 minutes. The cleared supernatants were incubated with pre-equilibrated GST Sepharose 4B affinity resin in a gravity flow column overnight at 4°C. GST-bound proteins were washed twice with 20 resin bed volumes of lysis buffer and then re-
535 equilibrated in TBS (150 mM NaCl, 50 mM Tris, 1 mM EDTA, 1 mM DTT, pH 7.2) at room temperature. The proteins were cleaved from the GST resin by incubation with PreScission Protease (GE Healthcare) overnight at 4°C.

Arc capsid assembly assay

Glutathione S-transferase-cleaved and purified dArc1 and dArc1^{Dcapsid} protein eluates were
540 concentrated to 2.5 mL using Vivaspin 10 kDa MWCO ultrafiltration spin columns (Cytiva). Protein concentration was measured using the DC Protein Assay (BioRad). Equal concentrations of dArc1 or dArc1^{Dcapsid} proteins were then applied to a Superdex 200 pg HiLoad 16/600 size exclusion column in Tris-Buffered Saline. Peak fractions were identified by chromatogram analysis and Coomassie staining, pooled, and concentrated. Following size exclusion, negative stain electron
545 microscopy grids were prepared for each sample at a protein concentration of 0.5 mg/mL.

Negative stain electron microscopy

For all negative stain electron microscopy samples, copper 200-mesh grids (Electron Microscopy Sciences) were glow-discharged for 25 seconds in a vacuum chamber at 30 milliamperes. A 3.5-microliter sample was applied to the grid for 45 seconds. Grids were washed twice, for five
550 seconds each, with 30-microliter water droplets, followed by one wash with one percent uranyl acetate on parafilm. Excess water and uranyl acetate were removed from the grid using filter paper, and a final droplet of uranyl acetate was added to the grids for 30 seconds. Excess uranyl acetate was then removed, and the grids were air-dried for 30 seconds. Imaging was performed using a JEOL-JEM 1400 electron microscope at 120 kilovolts. For each experiment, 15 images
555 were taken of each sample, following a standardized pattern of grid squares. Arc capsids ranging from 30 to 50 nanometers were manually counted using ImageJ/FIJI.

Statistical analysis

Measurements were taken from independent samples. All statistical analyses were performed using GraphPad Prism 10.3.1 (GraphPad Software, San Diego, CA). Individual tests for each
560 dataset are reported within the figure legends. Reported bar charts show the mean and the error bars as s.e.m. Reported line charts show the mean and the error bars as s.e.m. Reported violin

plots show the median (dashed line) and quartiles (dotted line). For all statistical analyses, significance was set at *p*-value of less than 0.05. In all figures the *p*-value is reported as *$p < 0.05$, **$p < 0.01$, ***$p < 0.001$, ****$p < 0.0001$. ns, non-significant.

565 **REFERENCES**

1. Shepherd, J. D. & Bear, M. F. New views of Arc, a master regulator of synaptic plasticity. *Nat. Neurosci.* **14**, 279–284 (2011).

2. Zhang, H. & Bramham, C. R. Arc/Arg3.1 function in long-term synaptic plasticity: Emerging mechanisms and unresolved issues. *Eur. J. Neurosci.* **54**, 6696–6712 (2021).

570 3. Pastuzyn, E. D. *et al.* The Neuronal Gene Arc Encodes a Repurposed Retrotransposon Gag Protein that Mediates Intercellular RNA Transfer. *Cell* **172**, 275-288.e18 (2018).

4. Ashley, J. *et al.* Retrovirus-like Gag Protein Arc1 Binds RNA and Traffics across Synaptic Boutons. *Cell* **172**, 262-274.e11 (2018).

5. Hantak, M. P., Einstein, J., Kearns, R. B. & Shepherd, J. D. Intercellular Communication in
575 the Nervous System Goes Viral. *Trends Neurosci.* **44**, 248–259 (2021).

6. Erlendsson, S. *et al.* Structures of virus-like capsids formed by the Drosophila neuronal Arc proteins. *Nat. Neurosci.* **23**, 172–175 (2020).

7. Cottee, M. A., Letham, S. C., Young, G. R., Stoye, J. P. & Taylor, I. A. Structure of *Drosophila melanogaster* ARC1 reveals a repurposed molecule with characteristics of
580 retroviral Gag. *Sci. Adv.* **6**, eaay6354 (2020).

8. Henriques, W. S. *et al.* The diverse evolutionary histories of domesticated metaviral capsid genes in mammals. *BioRxiv Prepr. Serv. Biol.* 2023.09.17.558119 (2023) doi:10.1101/2023.09.17.558119.

9. Awata, H. *et al.* The neural circuit linking mushroom body parallel circuits induces memory
585 consolidation in *Drosophila*. *Proc. Natl. Acad. Sci.* **116**, 16080–16085 (2019).

10. Mattaliano, M. D., Montana, E. S., Parisky, K. M., Littleton, J. T. & Griffith, L. C. The Drosophila ARC homolog regulates behavioral responses to starvation. *Mol. Cell. Neurosci.* **36**, 211–221 (2007).

11. Mosher, J. *et al.* Coordination between Drosophila Arc1 and a specific population of brain neurons regulates organismal fat. *Dev. Biol.* **405**, 280–290 (2015).

12. Guan, Z., Saraswati, S., Adolfsen, B. & Littleton, J. T. Genome-wide transcriptional changes associated with enhanced activity in the Drosophila nervous system. *Neuron* **48**, 91–107 (2005).

13. Tempel, B. L., Bonini, N., Dawson, D. R. & Quinn, W. G. Reward learning in normal and mutant *Drosophila*. *Proc. Natl. Acad. Sci.* **80**, 1482–1486 (1983).

14. Krashes, M. J. & Waddell, S. Aversive and Appetitive Olfactory Conditioning.

15. Lin, S. *et al.* Neural correlates of water reward in thirsty Drosophila. *Nat. Neurosci.* **17**, 1536–1542 (2014).

16. Shyu, W.-H. *et al.* Neural circuits for long-term water-reward memory processing in thirsty Drosophila. *Nat. Commun.* **8**, 15230 (2017).

17. Dudai, Y., Jan, Y. N., Byers, D., Quinn, W. G. & Benzer, S. dunce, a mutant of Drosophila deficient in learning. *Proc. Natl. Acad. Sci.* **73**, 1684–1688 (1976).

18. Krashes, M. J. *et al.* A Neural Circuit Mechanism Integrating Motivational State with Memory Expression in Drosophila. *Cell* **139**, 416–427 (2009).

19. Burke, C. J. & Waddell, S. Remembering Nutrient Quality of Sugar in Drosophila. *Curr. Biol.* **21**, 746–750 (2011).

20. Davis, R. L. SnapShot: Olfactory Classical Conditioning of Drosophila. *Cell* **163**, 524-524.e1 (2015).

21. Cognigni, P., Felsenberg, J. & Waddell, S. Do the right thing: neural network mechanisms of memory formation, expression and update in Drosophila. *Curr. Opin. Neurobiol.* **49**, 51–58 (2018).

22. Waddell, S. Reinforcement signalling in Drosophila; dopamine does it all after all. *Curr. Opin. Neurobiol.* **23**, 324–329 (2013).

23. Waddell, S. Neural Plasticity: Dopamine Tunes the Mushroom Body Output Network. *Curr. Biol.* **26**, R109–R112 (2016).

24. Jenett, A. *et al.* A GAL4-driver line resource for Drosophila neurobiology. *Cell Rep.* **2**, 991–1001 (2012).

25. Dana, H. *et al.* High-performance calcium sensors for imaging activity in neuronal populations and microcompartments. *Nat. Methods* **16**, 649–657 (2019).

26. Markow, T. A. The secret lives of Drosophila flies. *eLife* **4**, e06793 (2015).

27. Tatar, M., Post, S. & Yu, K. Nutrient control of Drosophila longevity. *Trends Endocrinol. Metab. TEM* **25**, 509–517 (2014).

28. Strilbytska, O. *et al.* Life-History Trade-Offs in Drosophila: Flies Select a Diet to Maximize Reproduction at the Expense of Lifespan. *J. Gerontol. A. Biol. Sci. Med. Sci.* **79**, glae057 (2024).

29. Moon, S. J. *et al.* Identification of high sugar diet-induced dysregulated metabolic pathways in muscle using tissue-specific metabolic models in Drosophila. *BioRxiv Prepr. Serv. Biol.* 2024.04.24.591006 (2024) doi:10.1101/2024.04.24.591006.

30. Pribbenow, C. & Owald, D. Skewing information flow through pre- and postsynaptic plasticity in the mushroom bodies of Drosophila. *Learn. Mem. Cold Spring Harb. N* **31**, a053919 (2024).

31. Yao, Z. & Scott, K. Serotonergic neurons translate taste detection into internal nutrient regulation. *Neuron* **110**, 1036-1050.e7 (2022).

32. Sahney, S., Benton, M. J. & Ferry, P. A. Links between global taxonomic diversity, ecological diversity and the expansion of vertebrates on land. *Biol. Lett.* **6**, 544–547 (2010).

33. Bayless, K. M. *et al.* Beyond Drosophila: resolving the rapid radiation of schizophoran flies with phylotranscriptomics. *BMC Biol.* **19**, 23 (2021).

34. Lander, E. S. *et al.* Initial sequencing and analysis of the human genome. *Nature* **409**, 860–921 (2001).

35. Gratz, S. J. *et al.* Genome Engineering of *Drosophila* with the CRISPR RNA-Guided Cas9 Nuclease. *Genetics* **194**, 1029–1035 (2013).

36. Gratz, S. J. *et al.* Highly Specific and Efficient CRISPR/Cas9-Catalyzed Homology-Directed Repair in *Drosophila*. *Genetics* **196**, 961–971 (2014).

37. Bischof, J., Maeda, R. K., Hediger, M., Karch, F. & Basler, K. An optimized transgenesis system for *Drosophila* using germ-line-specific φC31 integrases. *Proc. Natl. Acad. Sci.* **104**, 3312–3317 (2007).

38. Gibson, D. G. *et al.* Enzymatic assembly of DNA molecules up to several hundred kilobases. *Nat. Methods* **6**, 343–345 (2009).

39. Venken, K. J. T., He, Y., Hoskins, R. A. & Bellen, H. J. P[acman]: A BAC Transgenic Platform for Targeted Insertion of Large DNA Fragments in *D. melanogaster*. *Science* **314**, 1747–1751 (2006).

40. Dorkenwald, S. *et al.* Neuronal wiring diagram of an adult brain. Preprint at https://doi.org/10.1101/2023.06.27.546656 (2023).

41. Schlegel, P. *et al.* Whole-brain annotation and multi-connectome cell typing quantifies circuit stereotypy in *Drosophila*. Preprint at https://doi.org/10.1101/2023.06.27.546055 (2023).

42. Schindelin, J. *et al.* Fiji: an open-source platform for biological-image analysis. *Nat. Methods* **9**, 676–682 (2012).

43. Felsenberg, J., Barnstedt, O., Cognigni, P., Lin, S. & Waddell, S. Re-evaluation of learned information in Drosophila. *Nature* **544**, 240–244 (2017).

44. Jacob, P. F. & Waddell, S. Spaced Training Forms Complementary Long-Term Memories of Opposite Valence in Drosophila. *Neuron* **106**, 977-991.e4 (2020).

45. Jacobs, R. V. *et al.* Overlap and divergence of neural circuits mediating distinct behavioral responses to sugar. *Cell Rep.* **43**, 114782 (2024).

46. Abramson, J. *et al.* Accurate structure prediction of biomolecular interactions with AlphaFold 3. *Nature* **630**, 493–500 (2024).

47. Meng, E. C. *et al.* UCSF ChimeraX : Tools for structure building and analysis. *Protein Sci.* **32**, e4792 (2023).

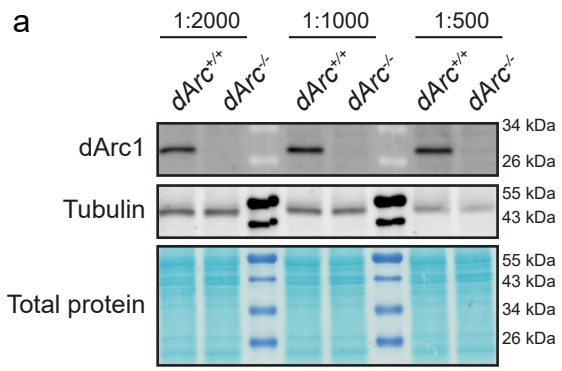
a
1:2000
1:1000
1:500
dArc+/+
dArc-/-
dArc+/+
dArc-/-
dArc+/+
dArc-/-
dArc1
Tubulin
Total protein
34 kDa
26 kDa
55 kDa
43 kDa
55 kDa
43 kDa
34 kDa
26 kDa

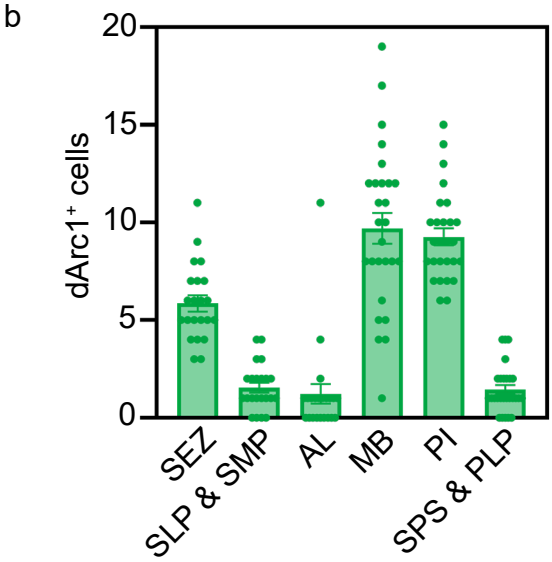
b
dArc1+ cells
20
15
10
5
0
SEZ
SLP & SMP
AL
MB
PI
SPS & PLP

Extended data figure 1.

(a) The expression of dArc1 protein in the adult fly head was determined by western blot using a custom rabbit antibody. Tubulin and total protein were used as loading controls.

(b) The localization of dArc1 positive cells was determined in the *dArc*$^{+/+}$ fly brain. SEZ, subeosophageal zone; SLP & SMP, superior lateral and superior medial protocerebrum; AL, antennal lobes; MB, mushroom body; PI, posterior inferior; SPS & PLP, superior posterior slope and posterior lateral protocerebrum.

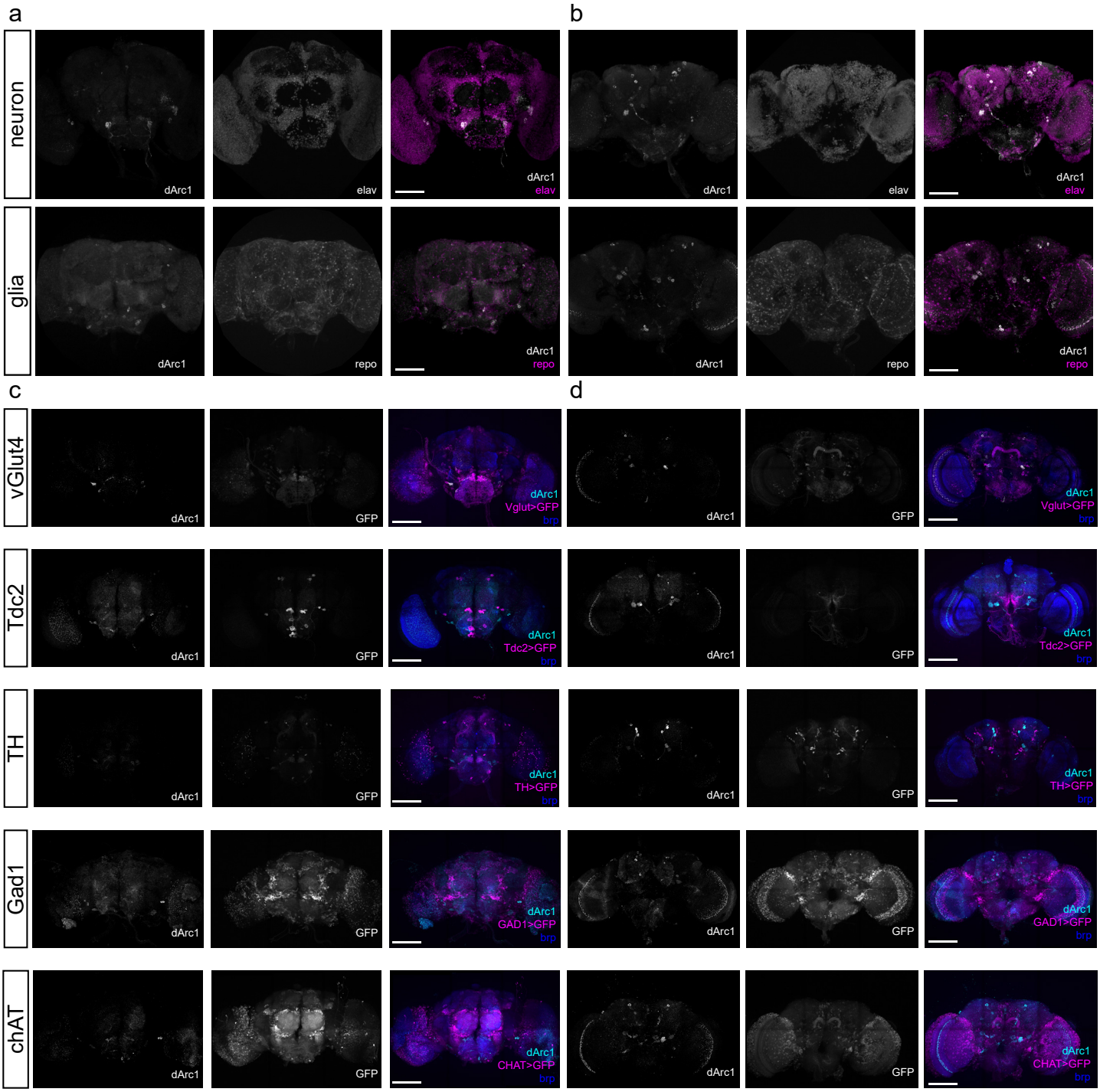
a
b
neuron
glia
dArc1
elav
repo
c
d
vGlut4
Tdc2
TH
Gad1
chAT
GFP
Vglut>GFP
Tdc2>GFP
TH>GFP
GAD1>GFP
CHAT>GFP
brp

Extended data figure 2.

(a) The brains of *dArc*$^{+/+}$ flies were immunostained using antibodies against the neuronal transcription factor elav (magenta) or glial marker repo (magenta), and dArc1 (white). Shown are the anterior and

(b) posterior views. Scale bars indicate 100 μm.

(c) The brains of *dArc*$^{+/+}$ flies expressing UAS-GFP in specified neurotransmitter subtypes (magenta) were immunostained using antibodies against dArc1 (cyan) and a neuropil marker brp (blue). *vGlut4-GAL4*: glutamatergic, *Tdc2-GAL4*: octopaminergic, *TH-GAL4*: dopaminergic, *Gad1-GAL4*: GABAergic, *chAT-GAL4*: cholinergic neurons. Shown are the anterior and

(d) posterior views. Scale bars indicate 100 μm.

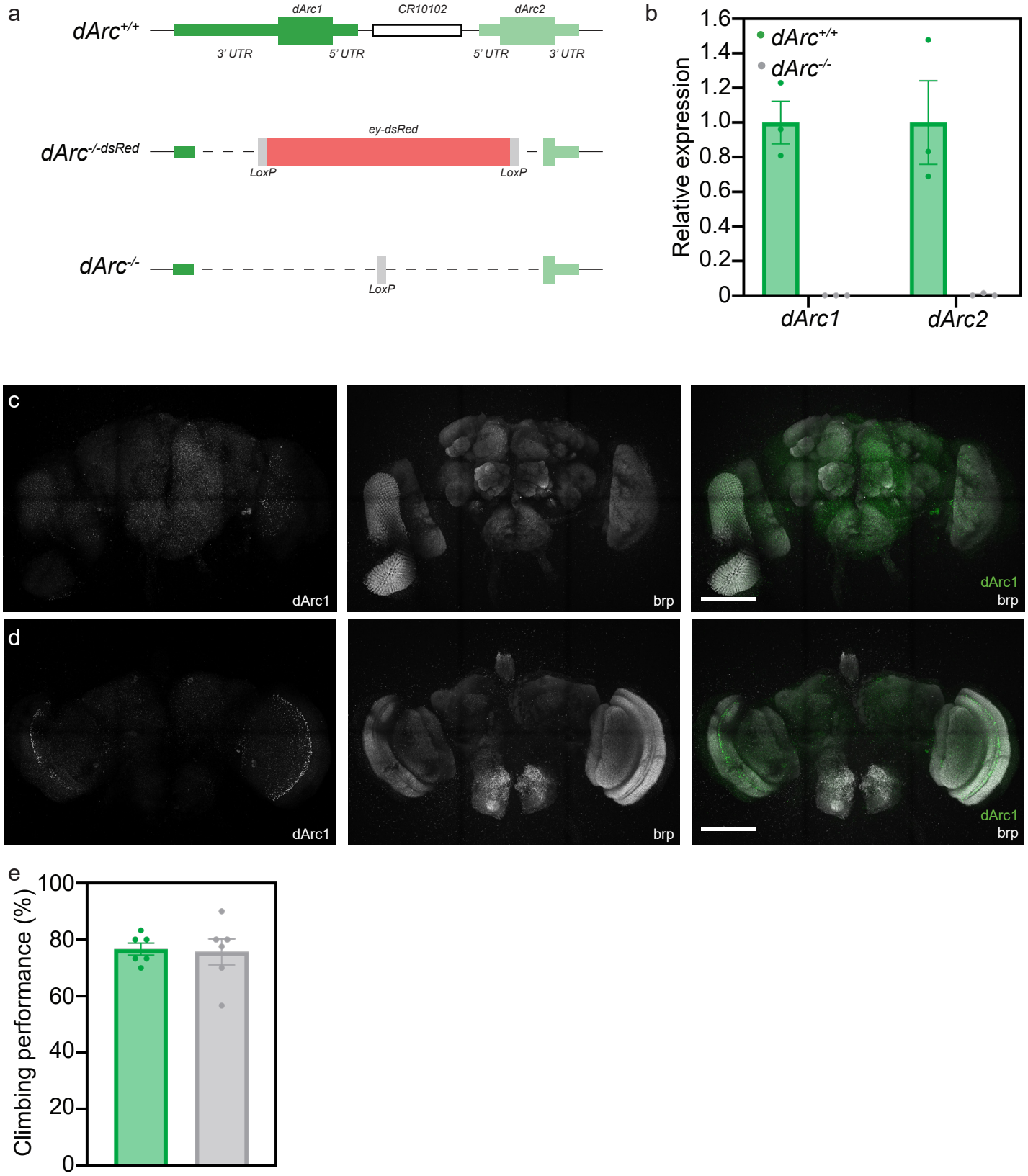
a
dArc+/+
dArc1
CR10102
dArc2
3' UTR
5' UTR
5' UTR
3' UTR
dArc-/-dsRed
ey-dsRed
LoxP
LoxP
dArc-/-
LoxP
b
Relative expression
1.6
1.4
1.2
1.0
0.8
0.6
0.4
0.2
0
dArc+/+
dArc-/-
dArc1
dArc2
c
dArc1
brp
dArc1
brp
d
dArc1
brp
dArc1
brp
e
Climbing performance (%)
100
80
60
40
20
0

Extended data figure 3.

(a) Schematic overview of the dArc genetic locus showing *dArc1* on the minus strand and *dArc2* on the plus strand flanking the *CR10102* pseudogene. The three genes were replaced by an ey-DsRed cassette using independent gRNAs targeting *dArc1* and *dArc2*. The ey-DsRed cassette was then removed using Cre recombinase and the available LoxP sites.

(b) The expression of *dArc1* and *dArc2* mRNA was determined by quantitative PCR (n = 3 replicates).

(c) Anterior view of a $dArc^{-/-}$ fly brain that was immunostained with dArc1 and Brp antibodies. Scale bar represents 100 µm.

(d) Posterior view of a $dArc^{-/-}$ fly brain that was immunostained with dArc1 and Brp antibodies. Scale bar represents 100 µm.

(e) The percentage of flies crossing the 7cm mark during the negative geotaxis assay (n ≥ 6 groups of flies, Unpaired t-test). Subjects were female.

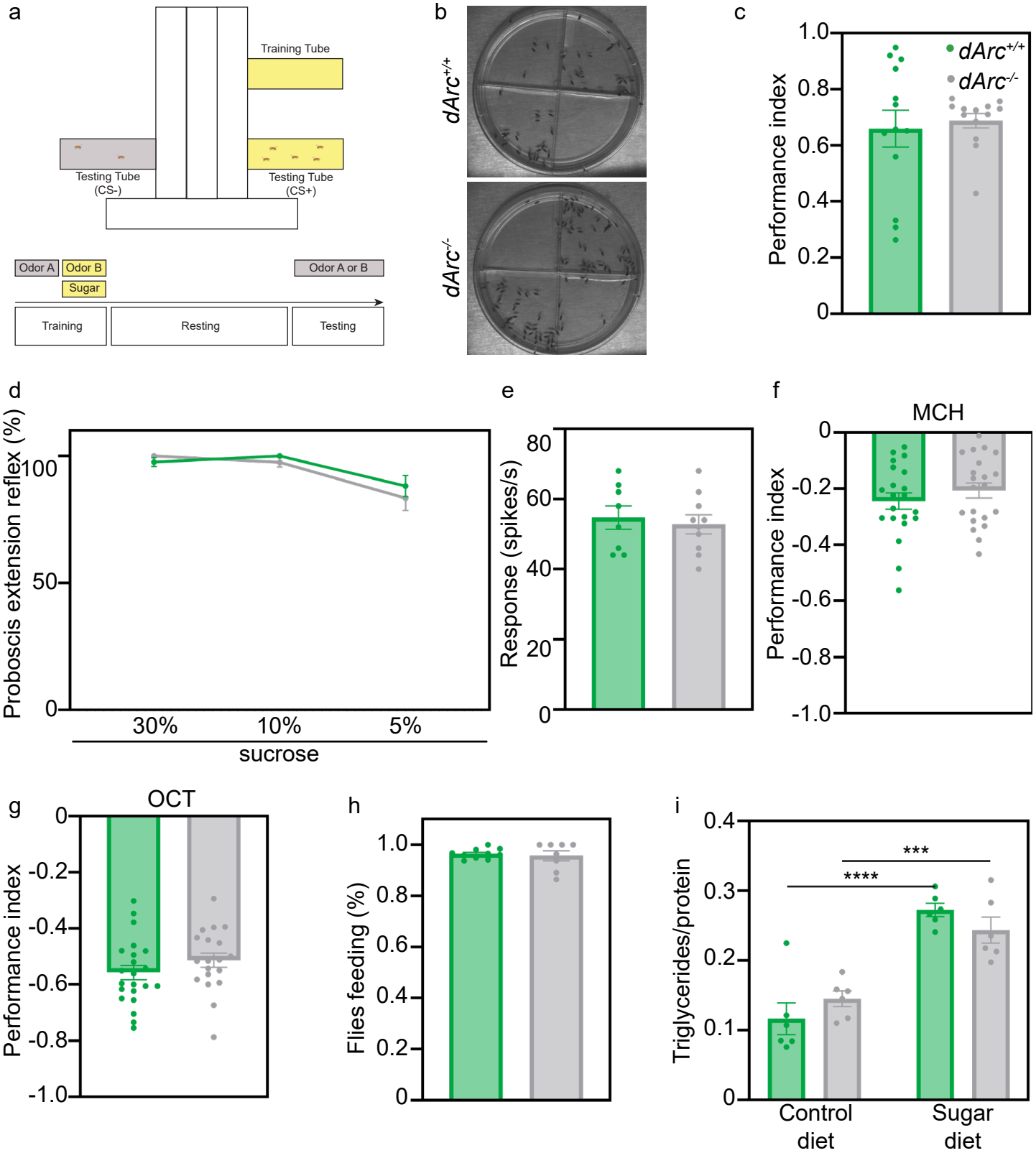
a
Training Tube
Testing Tube
(CS-)
Testing Tube
(CS+)
Odor A
Odor B
Sugar
Odor A or B
Training
Resting
Testing
b
dArc+/+
dArc-/-
c
Performance index
dArc+/+
dArc-/-
d
Proboscis extension reflex (%)
30%
10%
5%
sucrose
e
Response (spikes/s)
f
MCH
Performance index
g
OCT
Performance index
h
Flies feeding (%)
i
Triglycerides/protein
***
****
Control
diet
Sugar
diet

Extended data figure 4.

(a) A schematic of the *Drosophila* T-maze setup. Flies were initially exposed to an odor A without positive reinforcement (US-), followed by an odor B with a dried sucrose reward (US+). After a given rest period, flies were tested in a 2-choice assay between odor A (CS-) and B (CS+).

(b) Acuity for sugar of starved *dArc*$^{+/+}$ and *dArc*$^{-/-}$ flies was tested using a place-preference assay. Representative images are shown.

(c) The performance index for sugar acuity was determined for starved *dArc*$^{+/+}$ (green) and *dArc*$^{-/-}$ (grey) flies after 5 minutes (n ≥ 13 groups of flies, Unpaired t-test).

(d) The percentage of *dArc*$^{+/+}$ (green) and *dArc*$^{-/-}$ (grey) flies showing a proboscis extension reflex was determined in response to different concentrations of sucrose (n ≥ 20 flies, Two-way ANOVA).

(e) The electrophysiological responses of the sweet sensing sugar neurons of *dArc*$^{+/+}$ (green) and *dArc*$^{-/-}$ (grey) flies was determined after exposure to sucrose (n ≥ 8 flies, Unpaired t-test).

(f) The odor acuity of *dArc*$^{+/+}$ (green) and *dArc*$^{-/-}$ (grey) flies for 4-methylcyclohexanol (MCH) (n = 21 groups of flies, Unpaired t-test) and

(g) 3-octanol (OCT) was determined in a 2-choice assay for 2 minutes (n ≥ 19 groups of flies, Unpaired t-test).

(h) The fraction of flies feeding on the sucrose reward was determined for 2 minutes (n ≥ 8 groups of flies, Unpaired t-test).

(i) The metabolic responses of *dArc*$^{+/+}$ (green) and *dArc*$^{-/-}$ (grey) flies were determined after flies were fed a control or sugar diet. The ratio of triglycerides per protein is shown (n ≥ 6 groups of flies, Two-way ANOVA). Subjects were mixed sex. Bar charts are presented as means ± s.e.m.

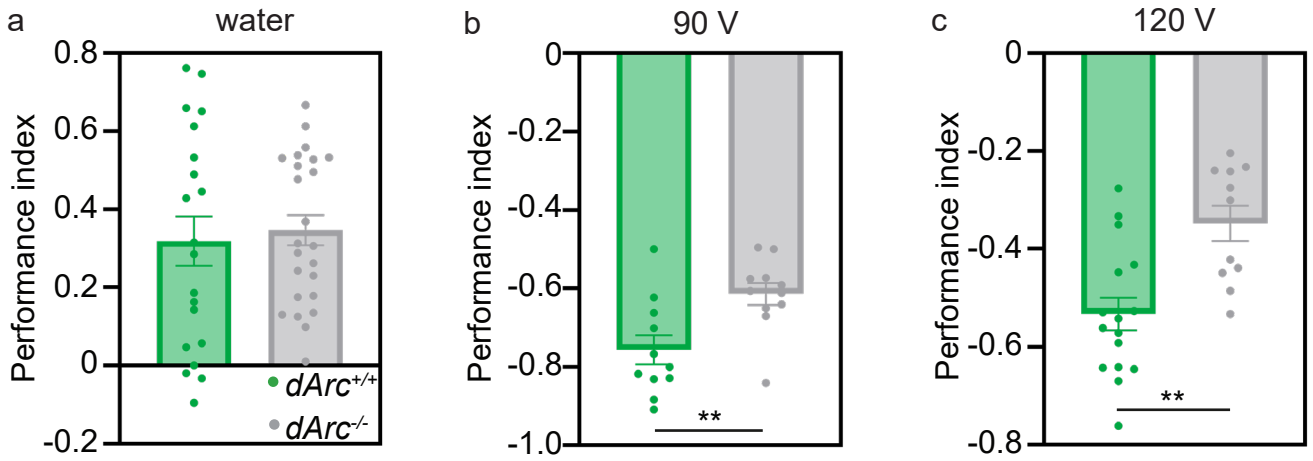
a
water
Performance index
0.8
0.6
0.4
0.2
0
-0.2
dArc+/+
dArc-/-
b
90 V
Performance index
0
-0.2
-0.4
-0.6
-0.8
-1.0
**
c
120 V
Performance index
0
-0.2
-0.4
-0.6
-0.8
**

Extended data figure 5.

(a) The performance index for water acuity was determined for *dArc*$^{+/+}$ (green) and *dArc*$^{-/-}$ (grey) flies in a 2-choice assay (n ≥ 20 groups of flies, Unpaired t-test).

(b) The performance index for electric shock acuity was determined for *dArc*$^{+/+}$ (green) and *dArc*$^{-/-}$ (grey) flies using 90V (n ≥ 11 groups of flies, Unpaired t-test) and

(c) 120V shocks using a 2-choice assay (n ≥ 11 groups of flies, Unpaired t-test). Subjects were mixed sex. Bar charts are presented as means ± s.e.m.

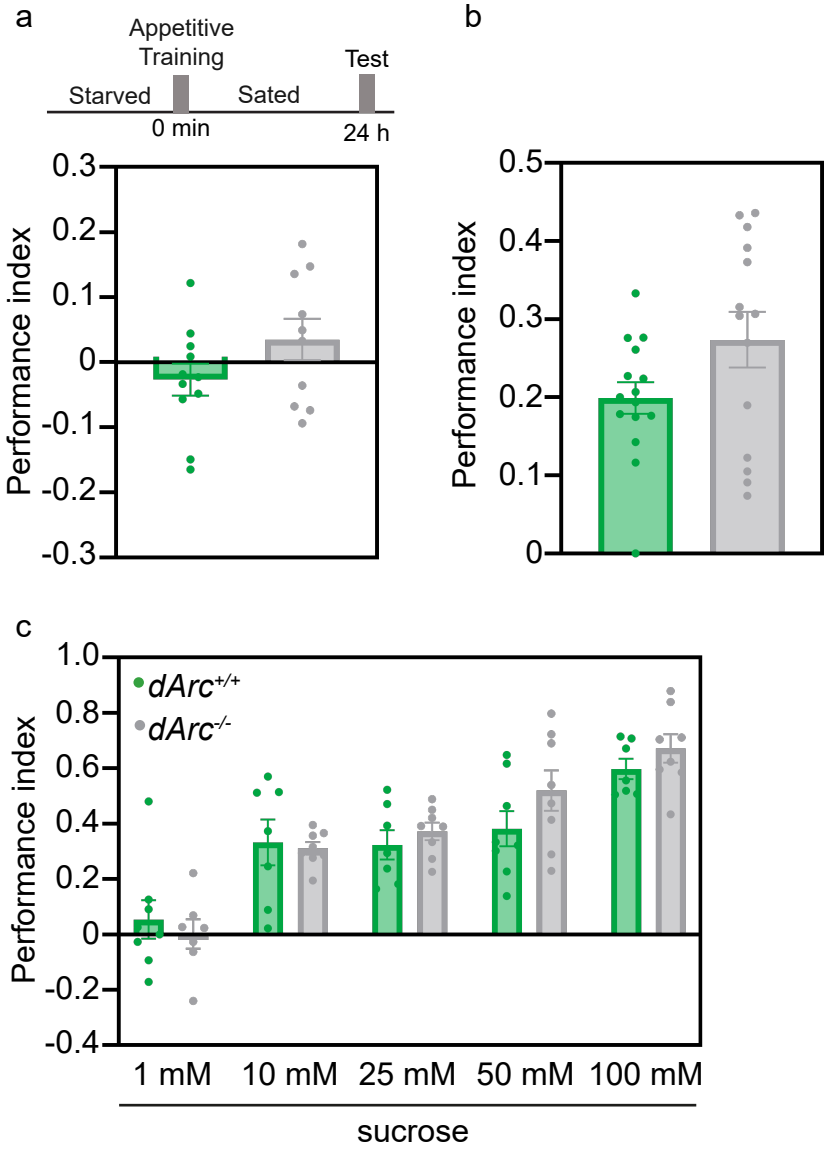
a
Appetitive
Training
Test
Starved
Sated
0 min
24 h
Performance index
0.3
0.2
0.1
0
-0.1
-0.2
-0.3
b
Performance index
0.5
0.4
0.3
0.2
0.1
0
c
Performance index
1.0
0.8
0.6
0.4
0.2
0
-0.2
-0.4
dArc+/+
dArc-/-
1 mM
10 mM
25 mM
50 mM
100 mM
sucrose

Extended data figure 6.

(a) Flies were starved for 20 hours and were subjected to an appetitive association paradigm using sugar. The flies were then fed ad libitum after training and tested after 24 hours. ($n \geq 10$ groups of flies, Unpaired t-test).

(b) The performance index for arabinose acuity was determined for starved *dArc*$^{+/+}$ (green) and *dArc*$^{-/-}$ (grey) flies using 100 mM arabinose in a place preference test ($n \geq 14$ groups of flies, Unpaired t-test).

(c) The performance index for sucrose acuity was determined for *dArc*$^{+/+}$ (green) and *dArc*$^{-/-}$ (grey) flies at different concentrations of sucrose in a place preference test ($n \geq 7$ groups of flies, Two-way ANOVA). Subjects were mixed sex. Bar charts are presented as means ± s.e.m.

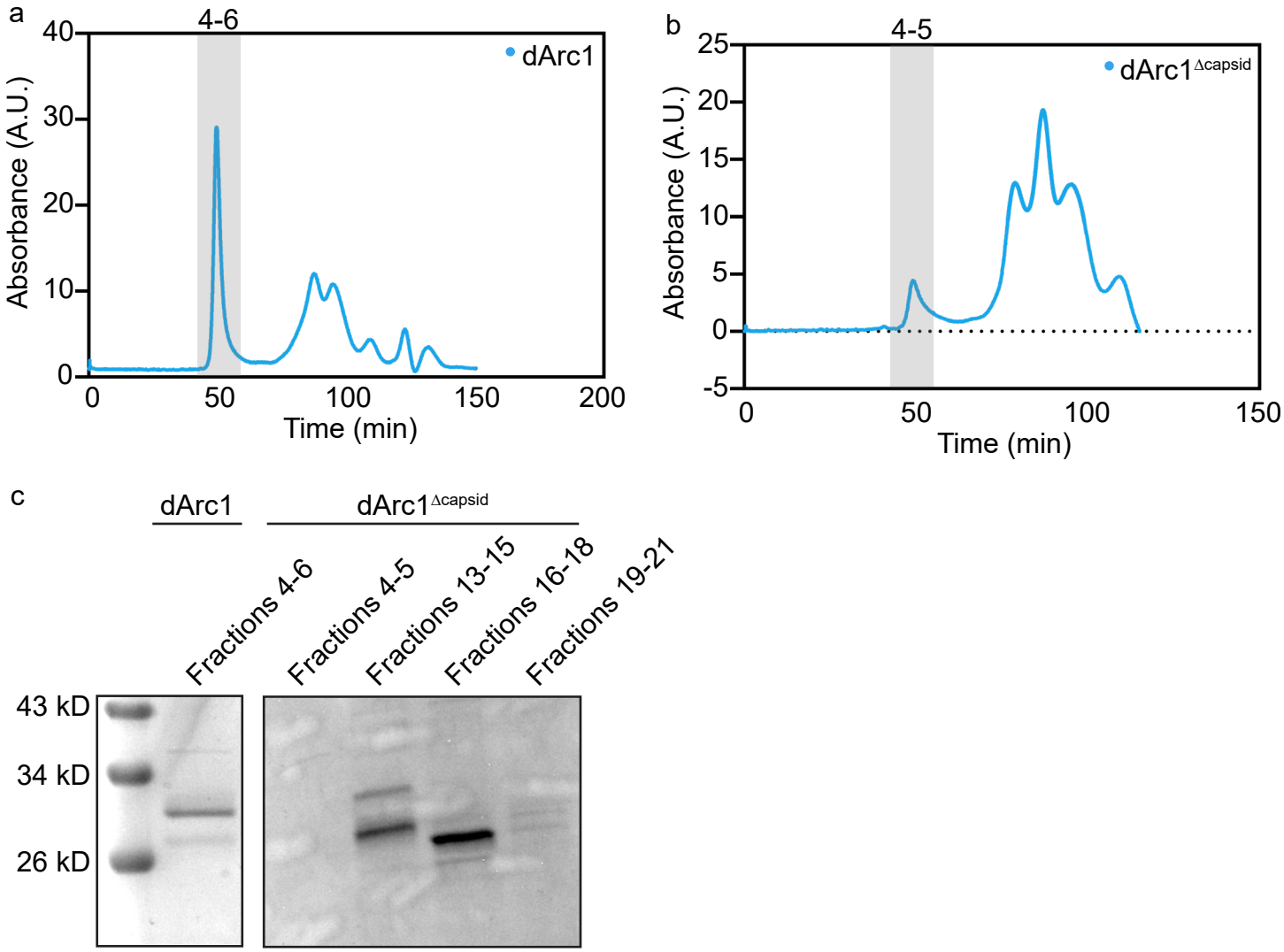
a
4-6
dArc1
Absorbance (A.U.)
Time (min)
b
4-5
dArc1Δcapsid
Absorbance (A.U.)
Time (min)
c
dArc1
dArc1Δcapsid
Fractions 4-6
Fractions 4-5
Fractions 13-15
Fractions 16-18
Fractions 19-21
43 kD
34 kD
26 kD

Extended data figure 7.

(a) Chromatogram of dArc1 purified protein showing the size exclusion chromatogram peaks selected for transmission electron microscopy.

(b) Chromatogram of dArc1$^{\Delta capsid}$ purified protein showing the size exclusion chromatogram peaks selected for transmission electron microscopy.

(c) Coomassie gel of the relevant peaks of purified dArc1 and dArc1$^{\Delta capsid}$ protein. Line charts are presented as a single purification.

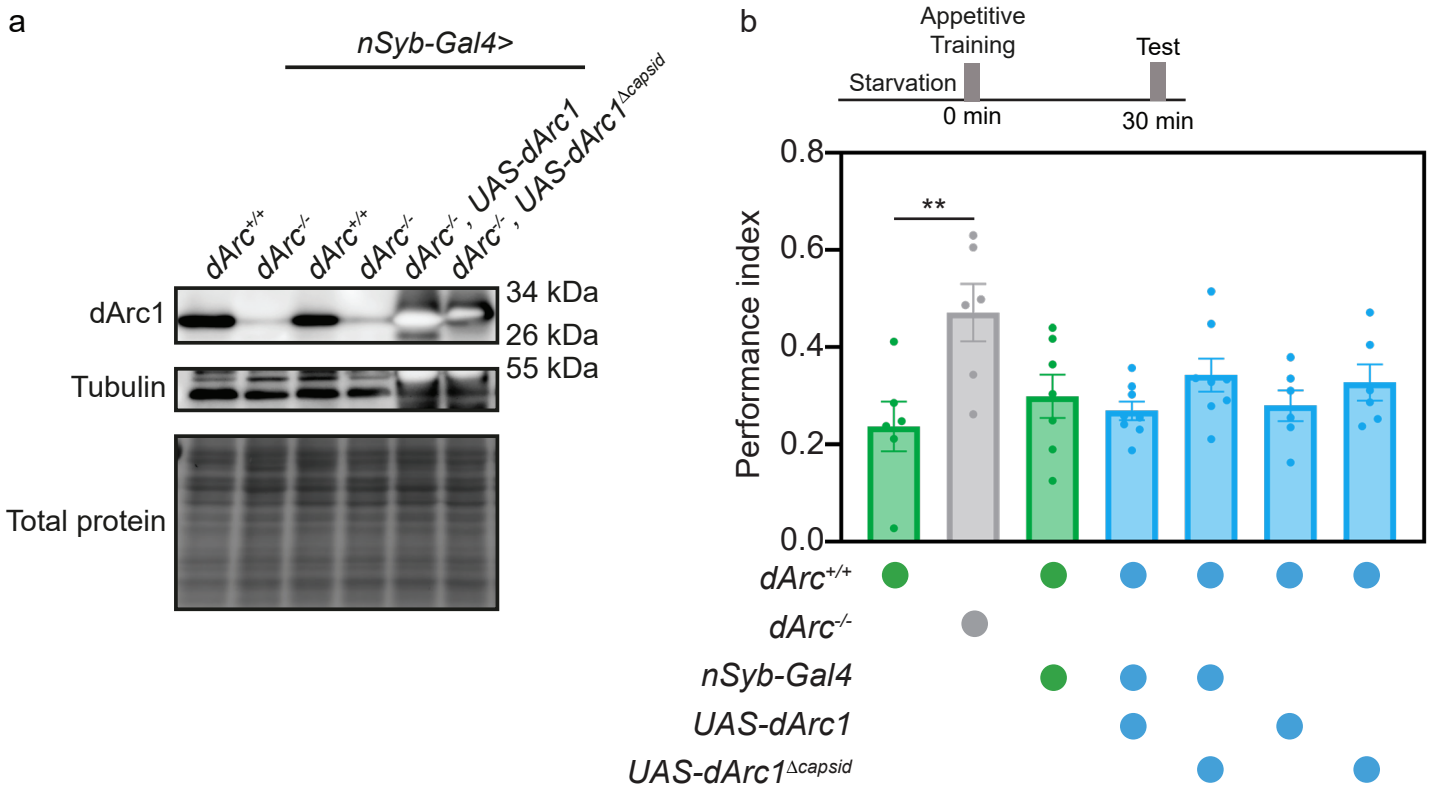
a
nSyb-Gal4>
dArc+/+
dArc-/-
dArc+/+
dArc-/-
dArc-/- , UAS-dArc1
dArc-/- , UAS-dArc1Δcapsid
dArc1
34 kDa
26 kDa
Tubulin
55 kDa
Total protein
b
Appetitive Training
Test
Starvation
0 min
30 min
Performance index
0.8
0.6
0.4
0.2
0.0
**
dArc+/+
dArc-/-
nSyb-Gal4
UAS-dArc1
UAS-dArc1Δcapsid

Extended data figure 8.

(a) Expression of dArc1 and dArc1$^{\Delta capsid}$ proteins in all neurons (nSyb-GAL4) of the fly in the *dArc*$^{-/-}$ background.

(b) Starved *dArc*$^{+/+}$ flies expressing dArc1 and dArc1$^{\Delta capsid}$ proteins in all neurons (*nSyb-GAL4*) were subjected to an appetitive association paradigm using sucrose and tested after 30 minutes (n ≥ 6 groups of flies, One-way ANOVA). Subjects were mixed sex. Bar charts are presented as means ± s.e.m.

EXTENDED DATA MATERIALS AND METHODS

Quantitative poly chain reaction (qPCR)

Quantitative PCR (qPCR) was performed as previously described[1]. Briefly, total RNA was isolated from different samples using a standard Trizol (Qiagen) and chloroform extraction protocol, followed by ethanol precipitation. The precipitated RNA was treated with recombinant DNase I (Roche). Single-stranded cDNA was synthesized using the high-capacity cDNA reverse transcription kit (Applied Biosystems). Gene expression levels were determined using the PowerUp SYBR Green Master Mix for qPCR (Applied Biosystems) and measured with the Quantstudio 3 real-time PCR system (Applied Biosystems). Data normalization was performed using four housekeeping genes. The stability of these housekeeping genes was first assessed across samples, and the most stable genes were selected to normalize the expression of the target genes. The primers used for the RT-qPCR analysis are listed in the Extended Table.

Western blot

Protein extracts were obtained using 1x RIPA buffer (50mM Tris-HCl (pH7.5), 1mM EDTA, 150mM NaCl, 0.1% SDS (sodium lauryl sulfate), 0.5% DOC (deoxycholic acid,sodium salt),1% Igepal CA-630 (NP40)). Protein extracts were mixed with 4X Laemmli buffer (40% glycerol, 250 mM Tris, 4% SDS, 50 mM DTT, pH 6.8) and heated at 95°C for five minutes. The proteins were separated by SDS-PAGE gel electrophoresis and transferred to a nitrocellulose membrane (GE Healthcare). Following transfer, membranes were briefly stained with Pierce™ Reversible Total Protein Stain and de-stained for total protein imaging. Membranes were blocked in 5% milk in 1X Tris-buffered saline-Tween (0.1%) (TBS; 10X: 152.3 mM Tris-HCl, 46.2 mM Tris-base, 1.5 M NaCl, pH 7.6) for 1 hour at room temperature. The blocked membranes were incubated with the primary antibody diluted in 5% milk in TBS-Tween overnight at 4°C. After incubation, membranes were washed five times for three minutes each with 1X TBS-Tween, followed by incubation with an HRP-conjugated secondary antibody (Jackson ImmunoResearch) in blocking buffer for one hour at room temperature. Membranes were then washed again three times for three minutes each time in 1X TBS-Tween, followed by two washes for three minutes in TBS. A chemiluminescence detection kit (Bio-Rad) was used to visualize the protein bands. Membranes were imaged using an Amersham ImageQuant 800 gel dock (Cytiva) and analyzed with ImageJ/Fiji (National Institutes of Health).

Negative geotaxis assay

Negative geotaxis assays were performed following previously described protocols[1]. Flies were anesthetized 24 hours before the experiment to allow for clipping their wings. Flies were allowed to recover from anesthesia for at least one full day. Each experiment was conducted on a group of ten flies with clipped wings. During the assay, vials containing the flies were tapped on a hard surface to ensure that all the flies fell to the bottom of the vial. Negative geotaxis performance was calculated based on the percentage of flies that climbed seven centimeters within 15 seconds. Biological replicates (groups of 7-10 flies) of each genotype were tested across three technical replicates, and the average performance of each replicate was reported.

Sensory acuity assays

Sensory acuity assays were performed on groups of 60 to 100 flies. In general, flies were selected prior to an experiment without sedation. For odor acuity assays, flies were given the choice to enter one of two tubes in a T-maze: one tube was scented with an odor (3-octanol or 4-methylcyclohexanol) while the other tube was unscented. Flies had two minutes to make a choice. For water acuity assays, flies were presented with a choice between a tube containing a piece of wet paper and another tube containing a piece of dry paper. Flies had two minutes to make a choice. For electric shock acuity assays, flies chose between two copper-lined tubes in a T-maze: one tube was electrified, and the other was not. Flies had two minutes to make a choice. For each assay, the number of flies in each tube was counted, and the performance index (PI) was calculated using the following formula: $PI = \frac{(\mathrm{US+}-\mathrm{US-})}{(\mathrm{US+}+\mathrm{US-})}$.

To determine the sugar acuity, flies were mouth pipetted into a dish divided into four quadrants: two quadrants were filled with a solution containing 1% agarose and the remaining two quadrants were filled with a solution containing 1% agarose and different concentrations of sucrose. Flies had five minutes to make a choice after which an image was taken. The number of flies were counted on the images, and the performance index (PI) was calculated based on the number of flies found in each quadrant and using the following formula: $PI = \frac{(\mathrm{US+}-\mathrm{US-})}{(\mathrm{US+}+\mathrm{US-})}$.

Proboscis extension reflex

Flies were starved for 18 to 24 hours in a vial with a dampened Kimwipe. The proboscis extension reflex in response to a sucrose solution of was measured as described in[3]. Briefly, a fly is fixed in a 200 µl yellow tip with a slant cut to reveal the head. Wicks dipped in sucrose solutions were

presented to the labellum of the fly until the fly extended its proboscis. Extension responses were scored manually under a stereomicroscope.

Sensory neuron electrophysiology

Sucrose responses from the labellar taste sensilla were recorded using the extracellular tip recording method, as previously described[2]. Male flies aged 6 to 10 days were cold-anesthetized, and their proboscis was immobilized by inserting the reference electrode containing Beadle-Ephrussi Ringer solution through the thorax into the labellum. Neuronal firing rates of the L4 sensilla were captured using a glass electrode (10–20 µm diameter) filled with either 100 mM or 500 mM sucrose mixed with an electrolyte (30 mM tricholine). The glass recording electrode was connected to the TastePROBE system (Syntech) and a IDAC acquisition controller (Syntech). Signals were amplified (10x), band-pass-filtered (99–3000 Hz), and sampled at 12 kHz. To analyze neuronal firing rates in response to sucrose stimulation, spikes were manually sorted, and the number of spikes per stimulation was determined using the Autospike software.

Sugar intake assay

Flies were first placed in a tube containing a dry piece of paper for 2 minutes. They were then transferred to a tube containing dried, blue-dyed sucrose paper for an additional 2 minutes. Immediately after exposure, flies were transferred to an Eppendorf tube and snap-frozen in liquid nitrogen. Flies were then visually scored for the presence of a blue proboscis or blue abdomen. Images of representative flies were captured using a Leica M165 FC microscope equipped with a Leica DMC 6200 camera and analyzed with the LAS X software.

Triglyceride measurements

Total triglycerides normalized to total proteins were measured as described previously[4]. Briefly, two flies per biological replicate were homogenized in a lysis buffer (140 mM NaCl, 50 mM tris-HCl (pH 7.4), and 0.1% Triton X-100) containing a protease inhibitor cocktail (Thermo Fisher Scientific). The lysate was then used to determine protein and triglyceride concentrations. Protein concentrations were measured using the Pierce bicinchoninic acid (BCA) assay (Thermo Fisher Scientific; absorbance at 562 nm), while triglyceride concentrations were measured using the LiquiColor Test (Stanbio; absorbance at 562 nm).

EXTENDED DATA REFERENCES

1. Bervoets, S. *et al.* Transcriptional dysregulation by a nucleus-localized aminoacyl-tRNA synthetase associated with Charcot-Marie-Tooth neuropathy. *Nat. Commun.* **10**, 5045 (2019).

2. Delventhal, R., Kiely, A. & Carlson, J. R. Electrophysiological Recording From Drosophila Labellar Taste Sensilla. *J. Vis. Exp.* 51355 (2014) doi:10.3791/51355.

3. Shiraiwa, T. & Carlson, J. R. Proboscis Extension Response (PER) Assay in Drosophila. *J. Vis. Exp.* 193 (2007) doi:10.3791/193.

4. May, C. E. *et al.* High Dietary Sugar Reshapes Sweet Taste to Promote Feeding Behavior in Drosophila melanogaster. *Cell Rep.* **27**, 1675-1685.e7 (2019).